Toxicology in Vitro 29 (2015) 1916–1931

Contents lists available at ScienceDirect

Toxicology in Vitro

journal homepage: www.elsevier.com/locate/toxinvit

High-content screening imaging and real-time cellular impedance monitoring for the assessment of chemical's bio-activation with regards hepatotoxicity

Ludovic Peyre [a,*], Georges de Sousa [a], Sylvie Barcellini-Couget [b], Anne-Pascale Luzy [c], Nathalie Zucchini-Pascal [a], Roger Rahmani [a,*]

[a] UMR 1331 TOXALIM (Research Centre in Food Toxicology), Institut National de la Recherche Agronomique (INRA), Laboratory of Xenobiotic's Cellular and Molecular Toxicology, 400 route des Chappes, BP 167, 06903 Sophia-Antipolis Cedex, France
[b] Odesia NeoSciences, INRA-Agrobiotech, 06903 Sophia-Antipolis, France
[c] Galderma R&D, 2400 Route des Colles, BP87, 06902 Sophia Antipolis Cedex, France

ARTICLE INFO

Article history:
Received 4 February 2015
Revised 29 June 2015
Accepted 30 July 2015
Available online 31 July 2015

Keywords:
Bio-activation
Cytotoxic assays
Drug-induced liver injury
Hepatotoxicity
High-content screening
Real-time cellular impedance

ABSTRACT

Testing hepatotoxicity is a crucial step in the development and toxicological assessment of drugs and chemicals. Bio-activation can lead to the formation of metabolites which may present toxicity for the organism. Classical cytotoxic tests are not always appropriate and are often insufficient, particularly when non metabolically-competent cells are used as the model system, leading to false-positive or false-negative results. We tested over 24 h the effects of eight reference compounds on two different cell models: primary cultures of rat hepatocytes and FAO hepatoma cells that lack metabolic properties. We performed inter-assay validation between three classical cytotoxicity assays and real-time cell impedance data. We then complemented these experiments with high-content screening (HCS) to determine the cell function disorders responsible for the observed effects. Among the different assays used, the neutral red test seemed to be well suited to our two cell models, coupled with real-time cellular impedance which proved useful in the detection of bio-activation. Indeed, impedance monitoring showed a high sensitivity with interesting curve profiles yet seemed unsuitable for evaluation of viability on primary culture. Finally, HCS in the evaluation of hepatotoxicity is likely to become an essential tool for use in parallel to a classical cytotoxic assay in the assessment of drugs and environmental chemicals.

1. Introduction

Biotransformation of xenobiotics is mostly performed in hepatocytes (De Sousa et al., 1991; Oesch and Diener, 1995; Shull et al., 1987). Unlike hepatomas (HepG2, Hep3B, Huh-7, etc.) or other commonly used indicator cell lines (CHO, fibroblasts, lymphoblasts, etc.), these highly differentiated cells express the majority of phase I and II metabolizing enzymes (Gerets et al., 2012; Hart et al., 2010; Wilkening et al., 2003). Thus, hepatocytes in primary culture constitute a reference model for *in vitro* toxicological studies and for pre-clinical evaluation of drugs (Guillouzo et al., 2007; Lecluyse and Alexandre, 2010). Xenobiotics target the hepatocytes where they either bring about direct toxicity or are bio-activated (Gómez-Lechón et al., 2010). Thus, hepatocytes are considered as an alternative in terms of predictability with respect to *in vivo* studies (Maier, 1988; Ponsoda et al., 1995, 2004).

One of the current challenges facing the cosmetic, pharmaceutical, chemical and food industries is sufficiently evaluating new molecules to ensure health and environmental safety. Increasing awareness of environmental and public concerns as well as recent restrictions in line with the evolution of ethics, have urged

Abbreviations: APAP, acetaminophen; AQ, amodiaquine; ATP, adenosine triphosphate; CBZP, carbamazepine; CI, cell index; CP, cyclophosphamide; CsA, cyclosporine A; DES, diethylstilbestrol; DILI, drug-induced liver injury; DMSO, dimethyl sulfoxide; ERY or E-mycin, erythromycin; FBS, fetal bovine serum; FS, furosemide; GSH, glutathione; HCS, high-content screening; IC_{50}, inhibitory concentration 50%; MTT, 3-(4,5-dimethylthiazol-2-yl)-2,5-diphenyltetrazolium bromide; NCI, normalized cell index; NRU, neutral red uptake; OM, oligomycin; PBS, phosphate buffered saline; RA, retinoic acid; REACH, registration, evaluation, authorization and restriction of chemicals; RTCA, real-time cell analyser; ROS, reactive oxygen species; SD, standard deviation; TBHP, tert-butyl hydroperoxide; XTT, 2,3-bis-(2-methoxy-4-nitro-5-sulfophenyl)-2H-tetrazolium-5-carboxanilide.

* Corresponding authors.
E-mail addresses: ludovic.peyre@sophia.inra.fr (L. Peyre), Roger.rahmani@sophia.inra.fr (R. Rahmani).

http://dx.doi.org/10.1016/j.tiv.2015.07.024
0887-2333/

researchers to develop alternative approaches to *in vivo* studies for predicting toxic potential of xenobiotics. Consequently, new effective *in vitro* alternative methods to animal testing are required, some examples of which have already been proposed (Prot and Leclerc, 2012; Rodrigues et al., 2013).

Exposure to chemicals and drugs was described to induce side effects, such as cell membrane alterations, disruption of apoptotic or necrotic processes, lipid peroxidation, immunoreaction, membrane transport perturbations, disruption of calcium homeostasis, increase in the levels of reactive oxygen species (ROS) or active metabolites, and lysosomal or mitochondrial dysfunctions (Kim et al., 2012; Larrey, 2009; Persson et al., 2013; Porceddu et al., 2012). These cellular alterations induce hepatotoxicity and drug-induced liver injury (DILI), the latter of which is responsible for about 13% of the cases of acute liver failure in the USA (Ostapowicz et al., 2002). This is a major issue that stops drug development at the pre-clinical and clinical stages (Hill et al., 2012) and is the main cause for drug withdrawals from the market (Suzuki et al., 2010). Indeed, DILI can manifest as acute (intrinsic hepatotoxicity) or chronic (idiosynchratic hepatotoxicity) liver disease (Bale et al., 2014) depending on genetic background, metabolism and environmental exposition.

Biotransformation and metabolic activation are processes that, by perturbation of the mitochondrial respiratory chain and consequential production of ROS, can lead to hepatotoxicity (Seeland et al., 2013). To measure this cytotoxicity, the European Union Reference Laboratory charged with providing approaches that do not involve animal testing (EURL-ECVAM), recommends the use of XTT as an improved alternative to the MTT test, combined with neutral red uptake (NRU) to measure and compare IC_{50}. Yet these current classical cytotoxic assays remain insufficient and have a low concordance with actual cases of human liver toxicity (Tolosa et al., 2012). Indeed, the existing tests to evaluate toxicity of chemicals are time-consuming, restricted to the measurement of metabolic activity and not always accurate. In this context, new methodologies using rapid and automated screening approaches to generate detailed and comparable toxicity date, need to be developed.

Here in this study, we aimed to compare the contribution of new innovative technologies with conventional toxicity assessment methods. We started the investigation by evaluating a group of selected compounds using the xCELLigence system (RTCA, real time cell analyser) in comparison with standard cytotoxic tests. This technique allowed us to monitor in real-time the overall cellular status of adherent cells in culture in dose-dependent kinetics, i.e. variation in the number of cells and in their cytomorphology (reflecting cytotoxicity, proliferation, mobility, ultra-structural modifications, etc.). The tests were conducted in a non-invasive environment, without the use of markers or stains, and are compatible for studying both early and late effects (Ke et al., 2011). This sensitive cellular assay is particularly suitable for studying the cellular toxicity of chemical entities or mixtures, and is appropriate for assessing rapid morphological changes (activation of membrane receptors) and mobility (Limame et al., 2012). Here we propose this technology, described previously by our team and others (Atienzar et al., 2011; Crépet et al., 2013; Martinez-Serra et al., 2014; Nawaz et al., 2014), as an alternative to the common tests currently employed to predict *in vitro* cytotoxicity in human hepatocytes.

In parallel to the use of the xCELLigence system, our investigations led us to develop new tests that incorporated the use of high content screening (HCS), a new technology designed to maximize productivity and efficiency. Our proposed test combines in one tool, measurements that can be made simultaneously by fluorescent microscopy, flow cytometry and microplate reader with a high speed analysis of the data, good specificity and sensitivity. This cytomics-based technology allows us the multiparametric evaluation of living cells in response to chemical stresses and can be used to create basic functional signatures in pharmacology and toxicology. The HCS can monitor cellular homeostasis in real-time using markers of apoptosis, autophagy, necrosis, proliferation, differentiation, oxidative stress and those of many other cell functions such as activation of certain pathways/receptors or drug influx/efflux, in order to screen and classify the hepatotoxicity potential of drugs depending on their mechanism of action (Tolosa et al., 2012). This method can be considered as a predictive *in vitro* cell-based assay, particularly useful during the early development stages, since it rapidly provides mechanistic information about the drug candidate and its predicted hepatotoxicity (Donato et al., 2012). Its implementation would reduce the dependence on animal models, as well as the cost and the time necessary to assess the developed drugs, and would promote increases in the number of biomarkers and compounds tested (Sirenko et al., 2014).

To study the role of metabolic activation in hepatotoxicity, eight drugs were tested (Table 1) on two cellular models: primary cultures of rat hepatocytes expressing all the metabolic enzymes necessary for biotransformation and which were previously used to detect drugs involved in DILI (Marchandeau and labbe, 2011), and FaO cells from murine hepatoblastoma which are deficient in most detoxification enzymes. Hence, we aimed at investigating the bio-activation process of selected compounds by comparing cytotoxicity results obtained from hepatic cells exhibiting or not xenobiotic biotransformation capabilities (i.e. primary cultured hepatocytes and FAO, respectively). In order to avoid interspecies variability, and to be as relevant as possible of prototypical studies conducted in toxicology, we choose to use rat as the reference species. The eight compounds were selected based on their toxicity profile and bio-activation properties, i.e. direct or indirect toxicity (linked to the biotransformation process), from lists in "the report and recommendations of ECVAM workshop 54" of products recommended for validation studies of alternative methods (Coecke et al., 2006). These can be found in the fourteenth updated edition of the bibliographic database of liver injuries and related drugs (Biour et al., 2004) or from the REACH concern products list. The cells were exposed to increasing concentrations of the tested compounds and comparative analyses of the cell viability data were performed based on four independent tests: the MTT, the neutral red uptake (NRU), the measurement of ATP content and a recent investigative tool, real-time cellular impedance monitoring. IC_{50} were calculated for each molecule after 24 h exposure and for each assessment method. Real-time cellular impedance monitoring was then performed to provide complementary data based on kinetics. Indeed, we assumed that if bio-activation was involved in hepatotoxicity, effects would be faster and IC_{50} lower in freshly isolated hepatocytes than in FaO cells. Finally, HCS allowed us to confirm the hepatotoxicity observed in response to the drugs used by showing the mechanisms involved.

2. Methods

2.1. Chemicals

Acetaminophen (PubChem CID:1983), amodiaquine (PubChem CID:64646), carbamazepine (PubChem CID:2554), cyclophosphamide (PubChem CID:22420), diethylstilbestrol (PubChem CID:448537), erythromycin (PubChem CID:12560), furosemide (PubChem CID:3440), retinoic acid (PubChem CID:444795), erythrosine B, neutral red, MTT (3-(4,5-dimethylthiazol-2-yl)-2,5-di phenyl tetrazolium bromide), bovine serum albumin and dimethyl sulfoxide (DMSO) were all purchased from the Sigma–Aldrich Chemical Company (Saint-Quentin Fallavier, France). Type CLS2

Table 1
Principal characteristics of the hepatotoxic drugs tested.

Molecule	Pharmacological use	Hepatotoxicity/mechanism of action	CYP metabolization	References
Acetaminophen	Analgesic–Antipyretic	OS, MD, RM, A	CYP2E1, CYP1A2, CYP2D6, CYP3A4	McGill and Jaeschke (2013)
Retinoic acid	Antiacneic	CG, D, A	CYP26A1/B1/C1 CYP2E1, CYP2S1, CYP2C, CYP3A4	Shmarakov et al. (2014)
Amodiaquine	Antimalaria–anti-inflammatory agent	OS, RM	CYP2C8	Tafazoli and O'Brien (2009)
Carbamazepine	Anticonvulsant–mood-stabilizing	RM	CYP1A, CYP2A, CYP2B, CYP2C, CYP3A	Higuchi et al. (2012)
Cyclophosphamide	Antineoplasic–Immunosuppressor	AM, RM, OS, PBAS	CYP1A1/2, CYP2B, CYP3A, CYP2C	Suzuki et al. (2008)
Diethylstilbestrol	Synthetic oestrogen	PBAS, PTGM	CYP7A1, CYP7B1, CYP8A1, CYP3A4, CYP2B10	Vega et al. (2014)
Erythromycin	Bacteriostatic–bacteriocide	OS, A, RM, PBAS	CYP3A	Ansede et al. (2010) and Lam et al. (2006)
Furosemide	Diurectic	CCI, LP, RM	CYP4B1	Qu et al. (2014)

A = Apoptosis.
AM = Antimitotic.
CCI = Cytosolic Calcium Increase.
CG = Cell Growth.
D = Differentiation.
LP = Lipid peroxidation.
MD = Mitochondria Dysregulation.
OS = Oxidative Stress.
PBAS = Perturbation of Bile Acid Synthesis/Secretion.
PTGM = Perturbation of Triglyceride Metabolism.
RM = reactive metabolite.

collagenase is from Roche Applied. William's E medium, penicillin/streptomycin, Trypsin/EDTA and fetal bovine serum are all from Invitrogen (Cergy Pontoise, France). Ethanol and acetic acid are from Prolabo. The human insulin is from Novordisk (Bagsvaerd, Denmark).

Nuclear fluorescent probe Hoechst 33342 (Ex/Em: 350/461), MitoSOX™ Red Mitochondrial superoxide indicator to assess oxidative stress (Ex/Em: 510/580), LysoTracker Green as lysosomal activity indicator (Ex/Em: 504/511) and ThiolTracker™ Violet also called Glutathione Detection Reagent (Ex/Em: 404/526) were obtained from Molecular Probes (Life Technologies, Saint Aubin, France). TMRE membrane potential sensor to evaluate mitochondrial activity (Ex/Em: 549/574) and intracellular calcium indicator Fluo-8™ AM (Ex/Em: 490/514) were from FluoProbes® (Interchim, France). Positive controls tert-butyl hydroperoxide (TBHP), cyclosporine A (CsA) and oligomycin (OM) were purchased from Sigma–Aldrich Chemical Company (Saint-Quentin Fallavier, France).

2.2. Cell culture

Rat hepatocytes in primary culture were freshly isolated from *rattus norvegicus* OFA male rats (ECACC) weighing between 180 and 200 g (Iffa Credo, L'isles d'Arbesle, France). All animals have received humane care in compliance with institutional guidelines. Hepatocytes were isolated and cultured according to the protocol of Berry and Friend (1969) and modified by De Sousa et al. (1991). Briefly, after isolation by collagenase perfusion, cell viability was determined using the erythromycin B test exclusion, giving at least 80% of viable cells to be considered acceptable. Then, about 30000 hepatocytes were plated on 96-well plates (25000 on E-plates RTCA) previously coated with Type 1 collagen, rehydrated and cultured in humidified atmosphere at 37 °C containing 95% O_2 and 5% CO_2 with medium I (william E medium, 10% FBS, 50 UI/ml penicillin, 50 μg/ml streptomycin and 0.1 UI/ml insulin) for 24 h. The medium is then replaced by another similar medium (medium II) but deprived of serum and supplemented with hydrocortisone hemisuccinate (1 μM) and bovine serum albumin (240 μg/ml).

FaO cells come from *rattus norvegicus* hepatoma (ECACC) and are sub-clones of the H4-11-E-C3 line (isolated from a Reuber H35 rat hepatoma). They were primary cultived in 75 cm^2 flasks in humidified atmosphere at 37 °C containing 95% O_2 and 5% CO_2 with medium A (COON'S supplemented with 5% of fetal bovine serum and penicillin/streptomycin respectively 50 UI/ml and 50 μg/ml). 45000 cells/well in classical 96-plates and 40000 cells per well in E-plates (RTCA) were seeded after coating with type I collagen. Cells were exposed to drugs at 80% of density.

Drugs were prepared as stock solution 200 times concentrated in DMSO. The final concentration in medium is 0.5%.

2.3. Viability tests

Viable cells were determined by measuring the conversion of the tetrazolium salt MTT 3-(4,5-dimethylthiazol-2-yl)-2,5-diphenyltetrazolium bromide, Sigma–Aldrich (Saint-Quentin Fallavier, France) to formazan induced by mitochondrial succinate dehydrogenase, as previously described (fautrel et al., 1991). Briefly, after 24 h of treatment, medium is removed, cells are washed with medium II and then incubated with 0.5 mg/ml MTT for 2 h at 37 °C. The water-insoluble formazan crystal was dissolved by adding 100 μl DMSO to each well and the absorbance was determined with a spectrophotometer at 570 nm (MR7000, Dynatech Laboratories, Inc., USA).

The neutral red uptake is based on transport and storage of the weakly cationic supravital dye in lysosomes. After 24 h of treatment, medium is removed, cells are washed with medium II and then incubated with the same medium supplemented with 50 μg/ml of neutral red dye. Plates are incubated for 3 h at 37 °C. Cells are washed with PBS and 100 μl/well of ethanol/acetic acid (50/1/49-v/v/v) is added. After shaking and homogenization, the absorbance was determined with a spectrophotometer at 550 nm (MR7000, Dynatech Laboratories, Inc., USA).

The ATP monitoring was used for the quantitative evaluation of proliferation and cytotoxicity of cultured mammalian cells. Under the manufacturer's recommendations (ATPlite, luminescence assay, PerkinElmer), cell culture medium is removed and cells are first washed with 100 μl/well of PBS before adding medium II. Then 50 μl/well of lysis buffer is added and plate is agitated for

5 min at 700 rpm in an orbital shaker. 50 µl of substrate solution is added and plate is one more time shook. Luminescence is then measured using a MicroBeta Wallac luminometer (EG&G Wallac).

2.4. Cell imaging microplate assays and cellomics – ArrayScan^{XTI} scanning details

Primary culture of rat hepatocytes were seeded at 30×10^3 cells/well in black 96-well cell culture plates, and allowed to attach overnight in a humidified incubator at 37 °C, 5% CO_2. Independently, five markers/indicators were used: the MitoSOX™ Red Mitochondrial superoxide indicator, the ThiolTracker™ Violet also called Glutathione Detection Reagent, the LysoTracker® Green Probe, the TMRE membrane potential sensor and the Fluo-8™ AM calcium indicator. The HCS staining probes were used according to the manufacturer's instructions. Briefly, cells were treated for 24 h with different concentrations of chemicals. Then the stock concentration fluorescent probes contained in DMSO were diluted in a serum and phenol-red free medium (except for the MitoSOX in a HANK's medium) at final concentrations of 5 µM for the MitoSOX, 25 nM for the TMRE, 20 µM for the GSH, 50 nM for the LysoTracker and 5 µM for the Fluo-8. To each well, 100 µl of the final solution was added and incubated with the nuclear marker Hoechst 33342 (2.5 µg/ml final) at 37 °C. The medium was changed and the plates were scanned with the ArrayScanXTI instrument (Cellomics Inc., Pittsburgh, USA). The detection was performed with the "compartmental analysis" bio-application (Cellomics Inc., Pittsburgh, USA). An example of segmentation is shown on supplementary data 1 to illustrate the automated analysis. The number of cells analyzed was fixed to 500 cells per well. An objective of 20× was used for the imaging analysis. The nuclear dye (Hoechst) was detected in channel 1 (excitation–emission filter set 365/515 nm). The 'objects' targeted for measurement were detected in channel 2. The Cellomics ArrayScanXTI output features "mean circ spot total intensity" and "mean circ total intensity" depending on the probe tested were used to analyze the scans. For each plate, the mean of the three control wells (0.5% DMSO) was used as a reference and rescaled to one. Each well value was expressed relative to this reference. A value of two meant a 2-fold induction of the fluorescent signal compared with the control value. TBHP (500 µM), CsA (10 µM) and OM (0.5 µg/ml) were used as positive control in this experiment.

2.5. Real-time cellular impedance

Real-time cellular impedance consists in measuring the electrical response of alive and intact cells. Data are presented as a measurement curve called "Cell Index" or CI, depending on time. This CI was calculated from a relative electric impedance change of the cell layer. It is representative of a global cellular state. A linear relationship has been established by the manufacturer between variations covered by adherent cells surface and changes in CI. This indicates a change of the cell density and/or a change in adhesion or cellular morphology. The CI measurements were performed in a 96 well-plate with 80% of their bottom surface covered with gold microelectrodes. This electric measurement is realized in a non invasive context, without any staining or cell coloration.

The real-time cell impedance analyzer (xCELLigence® system) was used according to the manufacturers' instructions (Roche Applied Science, Mannheim, Germany and ACEA Biosciences, San Diego, CA, USA). For the rat hepatocytes and the FaO cell line, 25×10^3 and 40×10^3 cells/well respectively were added to 96-well E-plates. Twenty-four hours later, cells were treated with different concentrations of chemicals in William's medium. Real-time cellular impedance was measured in each well (Cell Index values) and the signal was observed through the integrated software (RTCA Analyzer). To observe the influence of chemicals on cells in comparison with the DMSO control, the normalized cell index (NCI) was used, based on the last time point prior to compound addition. Each curve is representative of an experiment performed in triplicate (technical replicates). Data are given as the mean ± standard deviation and are representative of three independent and reproducible experiments.

2.6. Statistical analyses

Each experiment was repeated at least three times in duplicate or triplicate, depending of the assay. Data shown are the mean ± standard deviation (SD). The cytotoxicity IC_{50} values and graph were carried out with GraphPad Prism program (version 5.0 GraphPad software Inc. San Diego, CA, USA). To determine the statistically significant difference between two groups, a Student's t test was used (two-tailed, paired samples for means, and hypothesized difference of 0).

3. Results

3.1. Acetaminophen hepatotoxicity presented two distinct steps

Paracetamol or acetaminophen (APAP) is a derivative of para-amino-phenol that is metabolized by the body. In a state of overdose, it can lead to irreversible liver necrosis and liver failure (McGill and Jaeschke, 2013). In this study, this compound presented weak toxicity with a slow effect on rat hepatocytes and an IC_{50} up to 10 mM when estimated using standard cytotoxicity assays. Indeed, the estimated IC_{50} was 26.44 mM with MTT (Fig. 1A, Table 2), 12.63 mM with neutral red staining (Fig. 1B, Table 3) and 18.33 mM with ATP monitoring (Fig. 1C, Table 4). Real-time cellular impedance technology appeared to be the most sensitive among the four tests, giving an IC_{50} of 3.98 mM on rat hepatocytes (Fig. 1D, Table 5). Moreover, it revealed modulations of viability or cellular morphology from 2 mM (Fig. 1E), suggesting that APAP may have phenotypical impact on hepatocytes at lower concentrations. Interestingly, this observation is supported by the HCS results (Fig. 10) which revealed two phenomena. The first being an increase in intracellular calcium at concentrations between 2.8 and 10.7 mM which occurred in parallel to a dose-dependent increase in nuclear intensity at 3.9–7.6 mM, without modulation of the nuclear area. The second being a change in nuclear area, an important indicator of toxicity, at concentrations between 10.7 and 15 mM, which occurred in parallel to a decrease in the mitochondrial potential activity and an increase in oxidative stress. While all assays were effective at predicting toxicity at these high concentrations, the perturbations observed at lower doses (calcium concentration and nuclear intensity) indicate that hepatotoxicity could happen earlier, as suggested by the neutral red staining.

On FaO cells, the toxicity of APAP was in the same range (IC_{50} = 18.5–19.5 mM) as that obtained on rat hepatocytes when evaluated with ATP monitoring (Fig. 1C). Although a very low toxicity was similarly revealed on this model, with an IC_{50} globally up to 15 mM (fitting estimation), the MTT test (Fig. 1A) and the NRU (Fig. 1B) gave different results to those obtained on primary cultures of hepatocytes ($IC_{50/MTT}$ = 15.13 mM; $IC_{50/NRU}$ = 29.89 mM) suggesting that APAP exhibits a different toxicity profile depending on the model, likely linked to the presence of metabolic enzymes. Finally, the impedance curves showed that APAP increased the cell index at all tested concentrations (Fig. 1D and F), with a Gaussian curve-type profile reaching a maximum at 4 mM, reflecting a cytomorphological change.

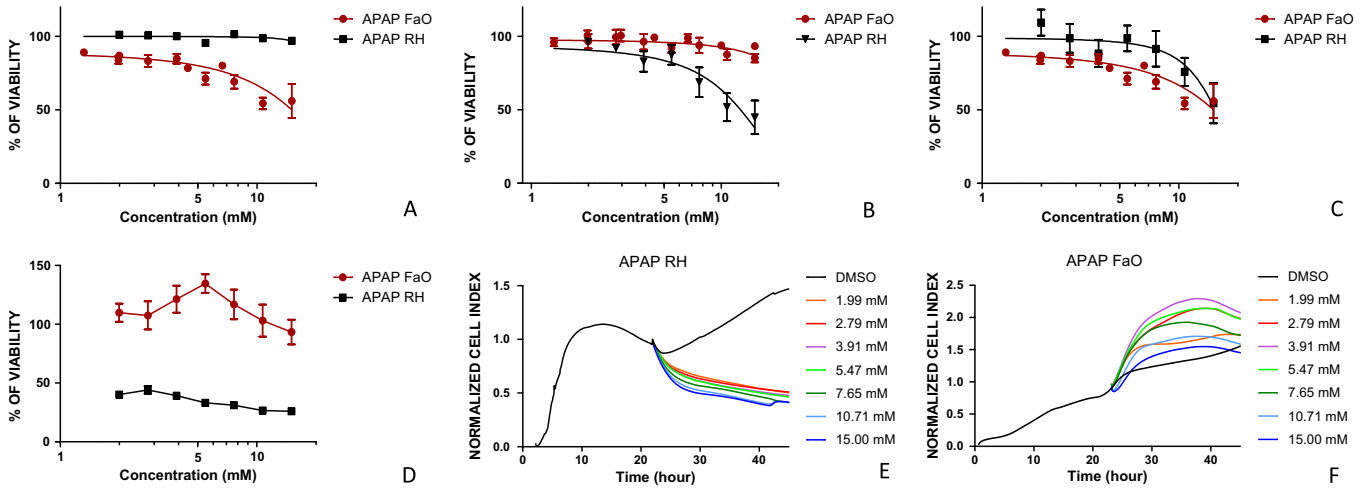

Fig. 1. Acetaminophen cytotoxicity monitoring of rat hepatocytes (RH) and FaO cell line. Cells were seeded onto 96-well plates and treated for 24 h with increasing concentrations of acetaminophen (APAP). Then, cell viability was assessed using MTT assay (A), NRU (B), ATP monitoring (C) and real-time impedance (D). (A–D) Results are presented as a percentage of viability over DMSO treatment and each value is the mean ± S.D. of three separate experiments. (E and F) Real-time impedance curves obtained from the xCELLigence system (Roche). Each curve was normalized just before compound addition on rat hepatocytes (E) or FaO cells (F) and represents an average of triplicate values.

Table 2
Cytotoxicity evaluated by MTT assay on rat hepatocytes and FaO hepatoma cells after 24 h treatment.

Molecule	IC_{50} RH (mM)	Interval 95%	IC_{50} FaO (mM)	Interval 95%
Acetaminophen	26.44	−0.18 to 53.06	15.13	13.75–16.51
Retinoic acid	0.102	0.095–0.110	0.052	0.049–0.055
Amodiaquine	0.028	0.024–0.032	0.0409	0.035–0.046
Carbamazepine	>1	–	>1	–
Cyclophosphamide	21.31	10.07–32.55	11.34	9.657–13.02
Diethylstilbestrol	0.185	0.165–0.205	0.0378	0.036–0.039
Erythromycin	1.21	1.14–1.28	3.385	2.935–3.835
Furosemide	6.526	6.024–5.363	11.33	10.08–12.59

Table 3
Cytotoxicity evaluated by neutral red uptake assay (NRU) on rat hepatocytes and FaO hepatoma cells after 24 h treatment.

Molecule	IC_{50} RH (mM)	Interval 95%	IC_{50} FaO (mM)	Interval 95%
Acetaminophen	12.63	10.76–14.5	29.89	22.98–36.8
Retinoic acid	0.052	0.048–0.055	0.046	0.041–0.051
Amodiaquine	0.012	0.011–0.014	0.014	0.013–0.015
Carbamazepine	2.197	1.793–2.601	>1	–
Cyclophosphamide	18.75	14.12–23.38	31.39	18.47–44.31
Diethylstilbestrol	0.135	0.121–0.149	0.0396	0.036–0.042
Erythromycin	0.924	0.868–0.979	2.727	2.655–2.799
Furosemide	4.922	4.481–5.363	9.122	8.902–9.342

Table 4
Cytotoxicity evaluated by ATP monitoring assay on rat hepatocytes and FaO hepatoma cells after 24 h treatment.

Molecule	IC_{50} RH (mM)	Interval 95%	IC_{50} FaO (mM)	Interval 95%
Acetaminophen	18.33	13.06–23.6	19.58	15.53–23.63
Retinoic acid	0.085	0.073–0.096	0.048	0.041–0.055
Amodiaquine	0.022	0.019–0.025	0.026	0.022–0.029
Carbamazepine	>1	–	>1	–
Cyclophosphamide	8.27	6.36–10.18	>8	–
Diethylstilbestrol	0.16	0.143–0.178	0.0429	Very wide
Erythromycin	0.871	0.804–0.937	3.00	Very wide
Furosemide	4.66	4.38–4.93	10.06	Very wide

Table 5
Cytotoxicity evaluated by real-time cell impedance monitoring on rat hepatocytes and FaO hepatoma cells after 24 h treatment.

Molecule	IC_{50} RH (mM)	Interval 95%	IC_{50} FaO (mM)	Interval 95%
Acetaminophen	3.98	2.48–5.48	ND	–
Retinoic acid	0.029	0.022–0.035	0.050	0.047–0.054
Amodiaquine	0.009	0.006–0.011	0.03	Graph
Carbamazepine	0.525	0.418–0.633	>1	–
Cyclophosphamide	2.607	1.616–3.599	>8	–
Diethylstilbestrol	0.057	0.039–0.075	0.0611	Very wide
Erythromycin	0.366	0.324–0.408	2.947	2.603–3.29
Furosemide	1.404	1.174–1.634	6.219	5.688–6.750

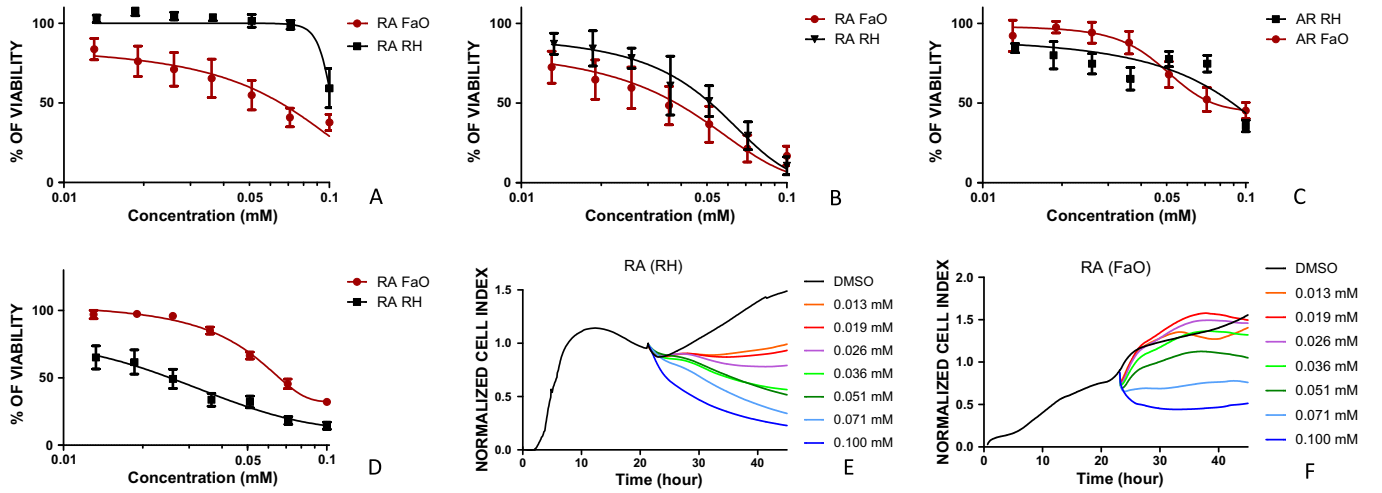

Fig. 2. Retinoic acid cytotoxicity monitoring of rat hepatocytes (RH) and FaO cell line. Cells were seeded onto 96-well plates and treated for 24 h with increasing concentrations of retinoic acid (RA). Then, cell viability was assessed using MTT assay (A), NRU (B), ATP monitoring (C) and real-time impedance (D). (A–D) Results are presented as a percentage of viability over DMSO treatment and each value is the mean ± S.D. of three separate experiments. (E and F) Real-time impedance curves obtained from the xCELLigence system (Roche). Each curve was normalized just before compound addition on rat hepatocytes (E) or FaO cells (F) and represents an average of triplicate values.

3.2. Retinoic acid hepatotoxicity is likely linked to mitochondrial disturbance

Retinoic acid (RA) is a metabolite of vitamin A and is involved in growth and differentiation during development. This molecule, known to be metabolized by the organism (Shmarakov et al., 2014), is used to treat acne as well as cancer. Here, we noted that RA was highly hepatotoxic towards rat hepatocytes with relatively slow kinetics (Fig. 2A–E). The IC_{50} ranged from around 29 μM for real-time cellular impedance, to 102 μM for the MTT test (Table 1). We found intermediate values using ATP content measurements (85 μM) and neutral red uptake (52 μM). When compared to HCS imaging results (Fig. 10) and to the other tests, data showed that MTT tended to under-evaluate the toxicity of retinoic acid whereas cellular impedance showed strong sensitivity, though probably not linked to hepatotoxicity, as suggested by the data set. Indeed, between 70 and 100 μM we detected a change in nuclear area and intensity, a decrease in the mitochondrial potential and of the intracellular calcium content (for the highest dose only), as well as a parallel increase in both oxidative stress and glutathione level. The HCS data were complemented by impedance curves which showed a dose-dependent effect of this drug on rat hepatocytes (Fig. 2E).

Our evaluations of RA on FaO cells showed comparable IC_{50} among the four assays ($IC_{50} \cong 50$ μM), with, when compared to hepatocytes, effects displaying similar and moderate kinetics (Fig. 2A–D). The impedance curves on FaO cells (Fig. 2F) revealed a decrease in the cell index at the following concentrations: 50, 70 and 100 μM. These data are in accordance with HCS results on hepatocytes and suggest that RA hepatotoxicity is detectable around 50–70 μM. In conclusion, ATP and neutral red uptake appear to be the most appropriate tests for this drug assessment whatever the cell model used. Moreover, only small differences were observed between IC_{50} estimated in hepatocytes versus those obtained in hepatoma cells, suggesting that metabolites are not involved in retinoic acid toxicity.

3.3. Amodiaquine hepatotoxicity: a two-step event with a particular profile

Amodiaquine is an antimalarial and anti-inflammatory drug which is metabolized in the liver but is also known to induce severe hepatic injury (Tafazoli and O'Brien, 2009). In our experiment, the classical cytotoxicity tests showed that amodiaquine is highly toxic towards hepatocytes (Fig. 3A–C), with IC_{50} between the 9 μM revealed using real-time cellular impedance (Fig. 3D and E, Table 5) and 28 μM using the MTT test (Fig. 3A, Table 2). The effects of this drug were found to have very fast kinetics regardless of the selected cytotoxicity test. Using HCS on this model, we identified two major events (Figs. 9 and 10). Firstly, we observed a decrease in the mitochondrial potential at concentrations in the range of 6.6–13 μM, which paralleled an increase in the lysosomal activity, suggesting an autophagic process secondary to an alteration of the mitochondrial status. Secondly, we noticed a high toxicity at concentrations between 18.2 and 50 μM, most likely linked to oxidative stress. Indeed, these concentrations provoked increases in reactive oxygen species, glutathione level and intracellular calcium, and modulated nuclear area and intensity. Mitochondrial

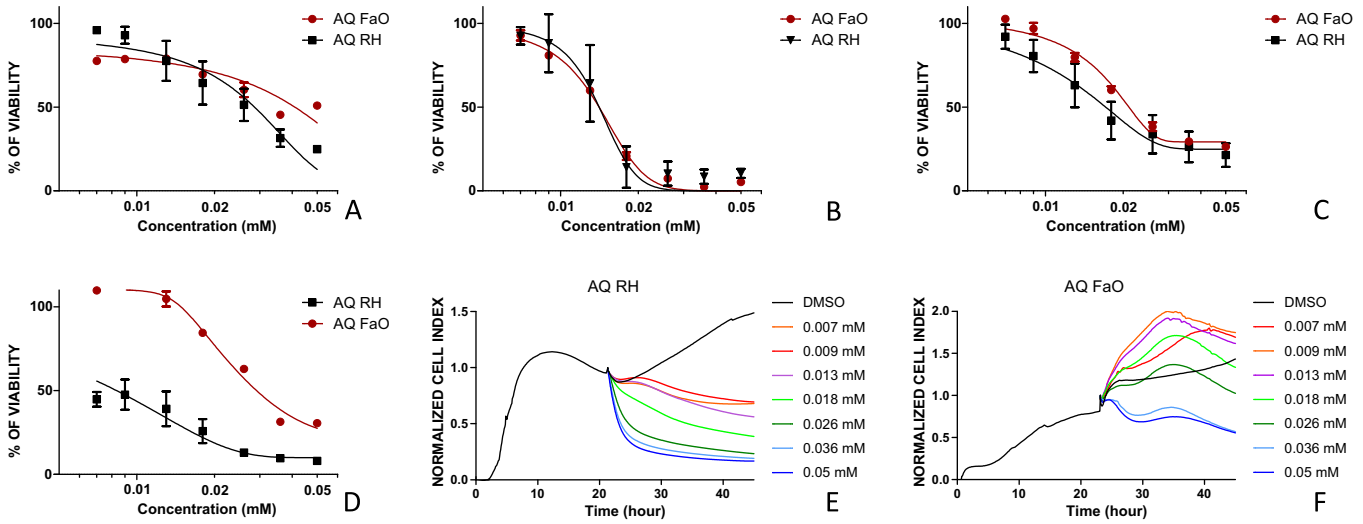

Fig. 3. Amodiaquine cytotoxicity monitoring of rat hepatocytes (RH) and FaO cell line. Cells were seeded onto 96-well plates and treated for 24 h with increasing concentrations of amodiaquine (AQ). Then, cell viability was assessed using MTT assay (A), NRU (B), ATP monitoring (C) and real-time impedance (D). (A–D) Results are presented as a percentage of viability over DMSO treatment and each value is the mean ± S.D. of three separate experiments. (E and F) Real-time impedance curves obtained from the xCELLigence system (Roche). Each curve was normalized just before compound addition on rat hepatocytes (E) or FaO cells (F) and represents an average of triplicate values.

activity also seemed to be highly affected with a decrease of 80% as compared to control conditions.

The IC_{50} in FaO cells was higher than that in hepatocytes according to the results of two of the four tests (Fig. 3A–D), with a maximum for the MTT test of 41 μM (Fig. 3A, Table 2) and with a minimum of 14 μM revealed using the NRU test (Fig. 3B, Table 3). Cytotoxicity was hence lower in this cell model than in the hepatocytes, suggesting that amodiaquine metabolites could be involved in hepatocyte cytotoxicity. Through the impedance curves (Fig. 3F), we observed an increase in the cell index during the first 12 h after treatment for concentrations ranging from 7 to 18 μM, a phenomenon often linked with changes in morphology and/or cell adhesion. These effects could be correlated with those observed using HCS, namely autophagy, oxidative stress and mitochondrial disturbances. Moreover, in contrast with the DMSO control, the cell index decreased at the high doses of 35 and 50 μM. Lastly, for all the concentrations tested and mostly at the lower doses, FaO cells showed a biphasic profile whereas hepatocytes only showed a dose-dependent effect, a difference in behavior which supports the hypothesis of detectable metabolism-related drug effects via impedance monitoring.

3.4. Carbamazepine does not exhibit a hepatotoxic profile

Carbamazepine (CBZP) is an anticonvulsant drug which is partially metabolized into active epoxide compounds in the liver and is suspected to induce hepatic injury (Higuchi et al., 2012). In our study, this drug did not appear to be hepatotoxic either in rat hepatocytes or in FaO cells, with tests performed up to the limit of dilution which is around 1 mM (Fig. 4A–D). As a result, we were unable to calculate an IC_{50} with either the MTT or the ATP test (Tables 2 and 4). Only neutral red assay provided an IC_{50} of 2.2 mM on rat hepatocytes (Table 3) while real-time cellular impedance detected an effect with a decrease in the NCI of 30–40% without dead cells observed in microscopy, suggesting a possible non-dose-dependent effect on hepatocyte phenotype in the absence of mortality (Fig. 4E). From HCS analysis, we noted a relatively weak antioxidant property which paralleled the decrease in lysosomal activity level between 260 and 714 μM (Fig. 10). We observed similar effects on FaO cells (Fig. 4F) with the cell index curves increasing in a biphasic manner for the lowest CBZP concentrations (133–510 μM). Without a direct correlation between oxidant stress and/or lysosomal activity with the modulation of the cellular impedance, we can only hypothesize on a possible non-toxic *in vitro* effect of CBZP on murine liver cells.

3.5. Cyclophosphamide is weakly hepatotoxic

As with the other drugs tested, cyclophosphamide (CP) is metabolized in liver. Indeed, its antineoplasic action is linked to the biotransformation processes but it can also lead to toxicity (Pirmohamed et al., 1992). Using classical cytotoxic tests on primary cultures of hepatocytes (Fig. 5A–D), we found no significant toxicity of this compound via MTT (IC_{50} = 21.31 mM) or neutral red tests (IC_{50} = 18.75 mM) whereas ATP monitoring (IC_{50} = 8.27 mM) and real-time cellular impedance detection (IC_{50} = 2.6 mM) showed a higher sensitivity with this drug. Our investigations on HCS (Fig. 10) then allowed us to identify two events. While mitochondrial potential decreased at low doses (1.1–2.9 mM), lysosomal activity increased, as already observed with amodiaquine. For higher concentrations (4.1–8 mM), we noted modulations of all the studied cell functions (except for the calcium content which remained stable). This high-dose toxicity probably correlates to oxidative stress as suggested by the modulations in levels of anion superoxide and GSH.

On FaO cells, none of the concentrations examined up to the limit of solubility showed any significant toxicity whatever the test used, as already observed on primary culture of hepatocytes (Fig. 5A–D and F). Consequently, we were unable to calculate the IC_{50} for example using the ATPu assay or with the real-time cellular impedance monitoring, which was estimated to be above 8 mM for this drug (Tables 4 and 5). Impedance results appeared to be non-dose-dependent and the weak differences observed supported weak toxic properties of this compound on the two cell models (Fig. 5E and F).

3.6. Diethylstilbestrol hepatotoxicity

Diethylstilbestrol (DES) is a synthetic oestrogen prescribed up until the early 1970s to counteract threats of premature birth or miscarriage. It is bio-transformed into reactive metabolites that lead to toxic effects (Vega et al., 2014). In our study, DES appeared

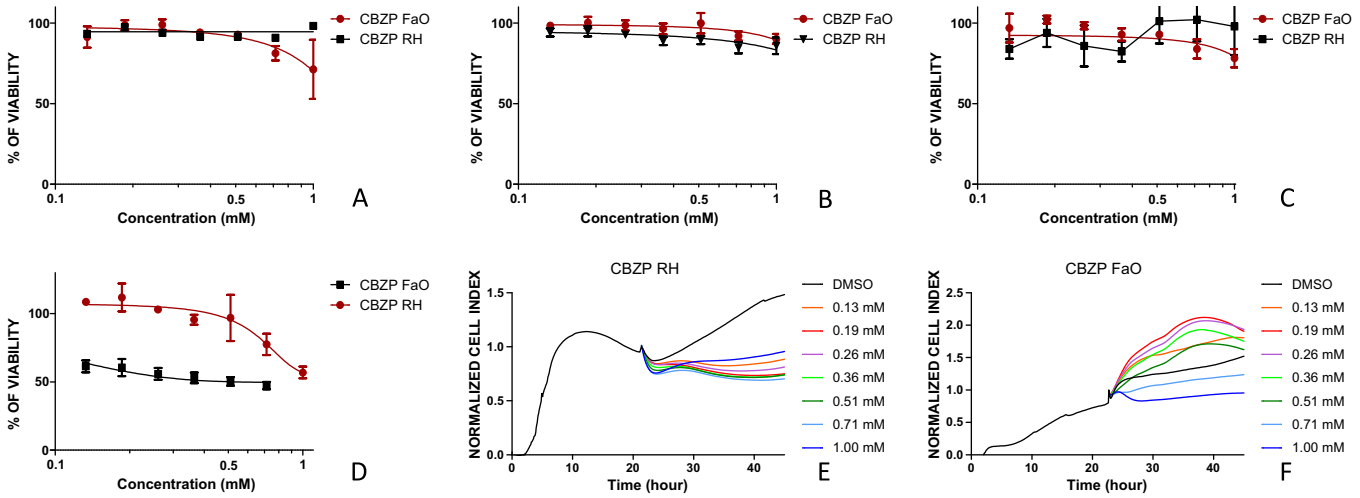

Fig. 4. Carbamazepine cytotoxicity monitoring of rat hepatocytes (RH) and FaO cell line. Cells were seeded onto 96-well plates and treated for 24 h with increasing concentrations of carbamazepine (CBZP). Then, cell viability was assessed using MTT assay (A), NRU (B), ATP monitoring (C) and real-time impedance (D). (A–D) Results are presented as a percentage of viability over DMSO treatment and each value is the mean ± S.D. of three separate experiments. (E and F) Real-time impedance curves obtained from the xCELLigence system (Roche). Each curve was normalized just before compound addition on rat hepatocytes (E) or FaO cells (F) and represents an average of triplicate values.

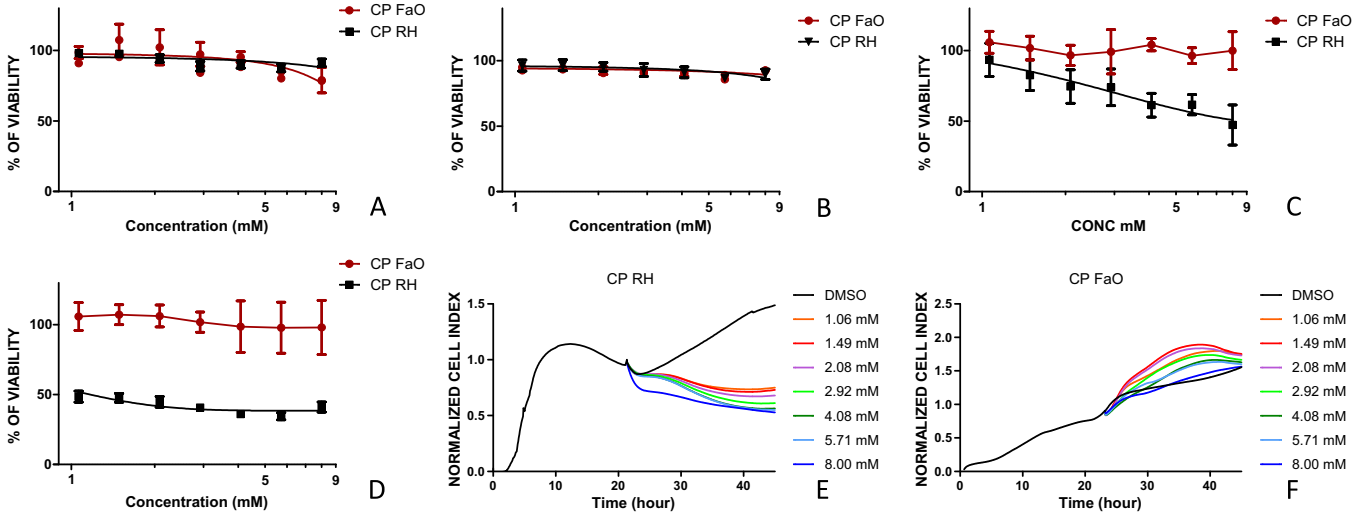

Fig. 5. Cyclophosphamide cytotoxicity monitoring of rat hepatocytes (RH) and FaO cell line. Cells were seeded onto 96-well plates and treated for 24 h with increasing concentrations of cyclophosphamide (CP). Then, cell viability was assessed using MTT assay (A), NRU (B), ATP monitoring (C) and real-time impedance (D). (A–D) Results are presented as a percentage of viability over DMSO treatment and each value is the mean ± S.D. of three separate experiments. (E and F) Real-time impedance curves obtained from the xCELLigence system (Roche). Each curve was normalized just before compound addition on rat hepatocytes (E) or FaO cells (F) and represents an average of triplicate values.

moderately toxic in comparison with the other drugs tested on rat hepatocytes, with a similar IC_{50} whatever the tests used (Fig. 6; IC_{50} = 135 μM with NRU, 185 μM with MTT and 160 μM with ATP). Cellular impedance showed a strong decrease in NCI with very fast dose-dependent kinetics (Fig. 6E). Thus, this compound seems able to deregulate most of the cell functions evaluated (Figs. 9 and 10). Indeed, in the range of 74–400 μM, DES increased GSH level in a dose-dependent manner (supplementary data 2 and 3), whereas mitochondrial potential rapidly and strongly decreased to reach a 0.2-fold induction for five of the seven doses used. The HCS technology suggested that DES could be toxic from 74 μM, a concentration at which we observed the increase in nuclear intensity with a parallel decrease in nuclear area. Interestingly, at this concentration the DES firstly strongly increased oxidative stress by 3-fold, before strongly decreasing the production of ROS to match the level of mitochondrial activity. Finally, DES exerted a negative effect on lysosomes by decreasing their activity, thus making the NRU test the least appropriate for use to assess this drug.

DES showed a higher toxicity in FaO cells than in hepatocytes, with an IC_{50} around 40 μM for the classical tests and 60 μM for real-time cellular impedance (Fig. 6A–D; Tables 2–5). This would suggest that bio-activation is not involved in DES toxicity; in other words, the hepatic metabolites are less toxic than the parent compound alone. The effects also displayed very fast kinetics, especially at high doses. On comparing the impedance curve profiles between the two cell models (Fig. 6F), we first noted a dose-dependent effect in hepatocytes with low cell index at high concentrations. On FaO cells on the other hand, the profile was different, with an increase in NCI for concentrations under 46 μM and

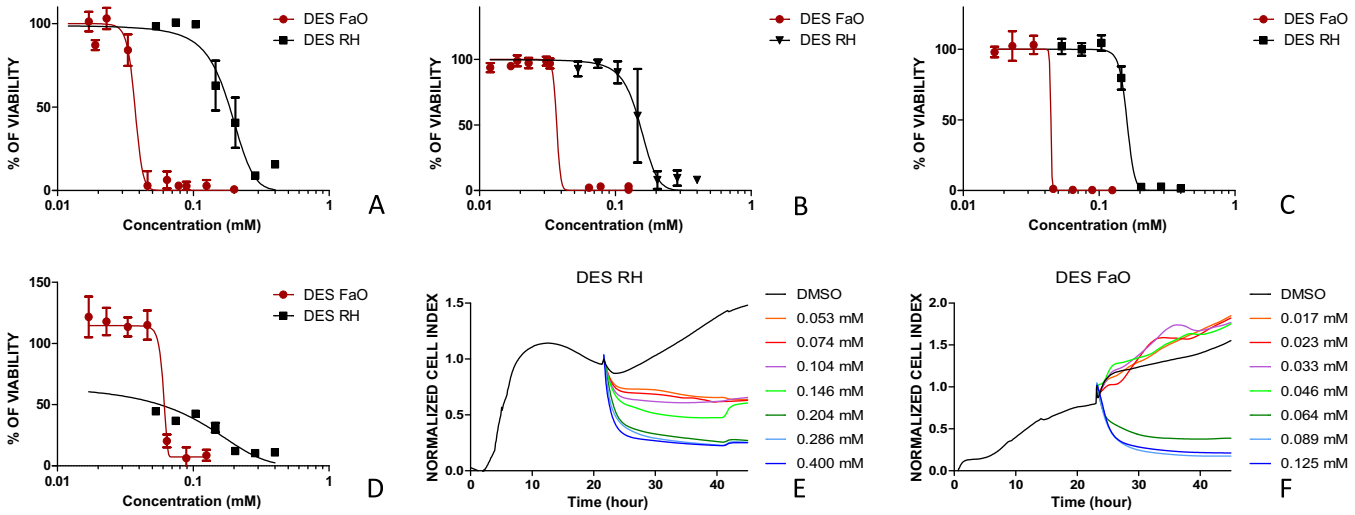

Fig. 6. Diethylstilbestrol cytotoxicity monitoring of rat hepatocytes (RH) and FaO cell line. Cells were seeded onto 96-well plates and treated for 24 h with increasing concentrations of diethylstilbestrol (DES). Then, cell viability was assessed using MTT assay (A), NRU (B), ATP monitoring (C) and real-time impedance (D). (A–D) Results are presented as a percentage of viability over DMSO treatment and each value is the mean ± S.D. of three separate experiments. (E and F) Real-time impedance curves obtained from the xCELLigence system (Roche). Each curve was normalized just before compound addition on rat hepatocytes (E) or FaO cells (F) and represents an average of triplicate values.

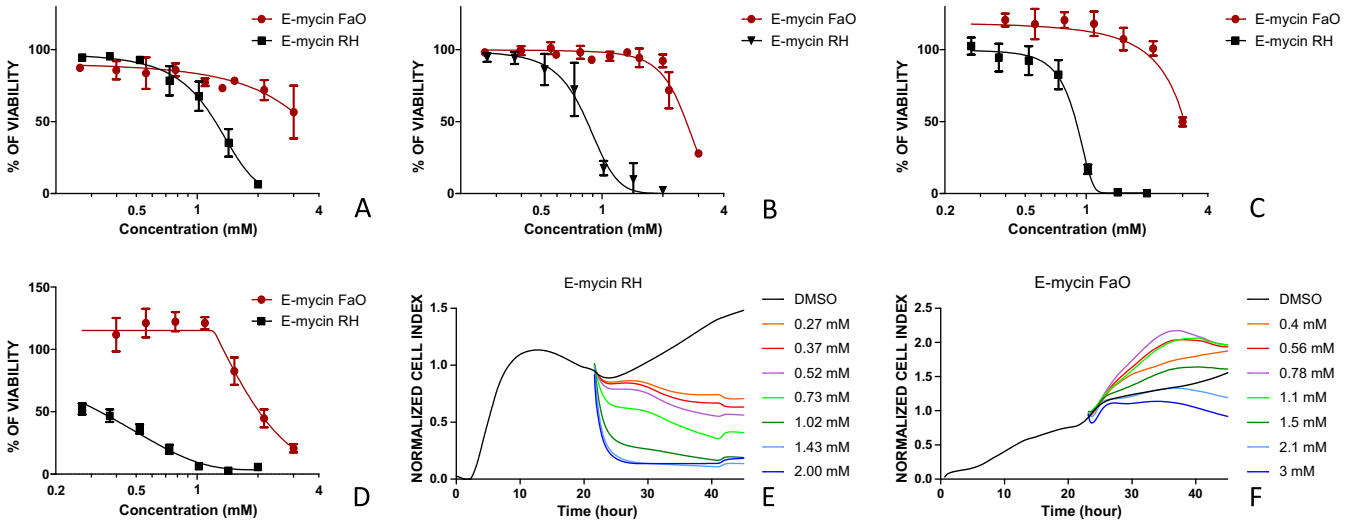

Fig. 7. Erythromycin cytotoxicity monitoring of rat hepatocytes (RH) and FaO cell line. Cells were seeded onto 96-well plates and treated for 24 h with increasing concentrations of erythromycin (E-mycin). Then, cell viability was assessed using MTT assay (A), NRU (B), ATP monitoring (C) and real-time impedance (D). (A–D) Results are presented as a percentage of viability over DMSO treatment and each value is the mean ± S.D. of three separate experiments. (E and F) Real-time impedance curves obtained from the xCELLigence system (Roche). Each curve was normalized just before compound addition on rat hepatocytes (E) or FaO cells (F) and represents an average of triplicate values.

a strong decrease for doses between 64 and 125 µM. At higher concentrations, DES was too toxic on this model, explaining our use of lower doses for this drug.

3.7. Erythromycin hepatotoxicity: two independent steps for two potential effects

Erythromycin (ERY or E-mycin) belongs to the macrolide bacteriostatic and bactericide family. Biotransformation occurs mainly in the liver where the metabolites strongly inhibit cytochrome P450 inducing drug–drug interaction and liver injury (Lam et al., 2006). In our experiments on rat hepatocytes, ERY was toxic at high concentrations (Tables 2–5) with fast kinetics (Fig. 7A–C) and similar hepatoxicity whatever the test used (MTT, IC_{50} = 1.2 mM; NRU, IC_{50} = 0.92 mM; ATP, IC_{50} = 0.87 mM). Only real-time cellular impedance (Fig. 7D and Table 5) led to a lower value and to a more sensitive result (IC_{50} = 0.36 mM), with a dose-dependent and sinusoidal profile (Fig. 7E). In parallel, we noted that ERY induced an important increase in the lysosomal activity (10-fold) which decreased progressively with increasing concentration of ERY (Figs. 9 and 10). We were unable to detect such a modulation at concentrations above 1.43 mM. However, in the range of 372–729 µM, we observed changes in nuclear area and intensity, a decrease in mitochondrial potential of about 60%, an increase in oxidative stress and GSH level, and finally an increase in intracellular calcium at concentrations above 1 mM.

On FaO cells, ERY was weakly toxic, with similar IC_{50} values (around 3 mM) whatever the end-point, suggesting that the

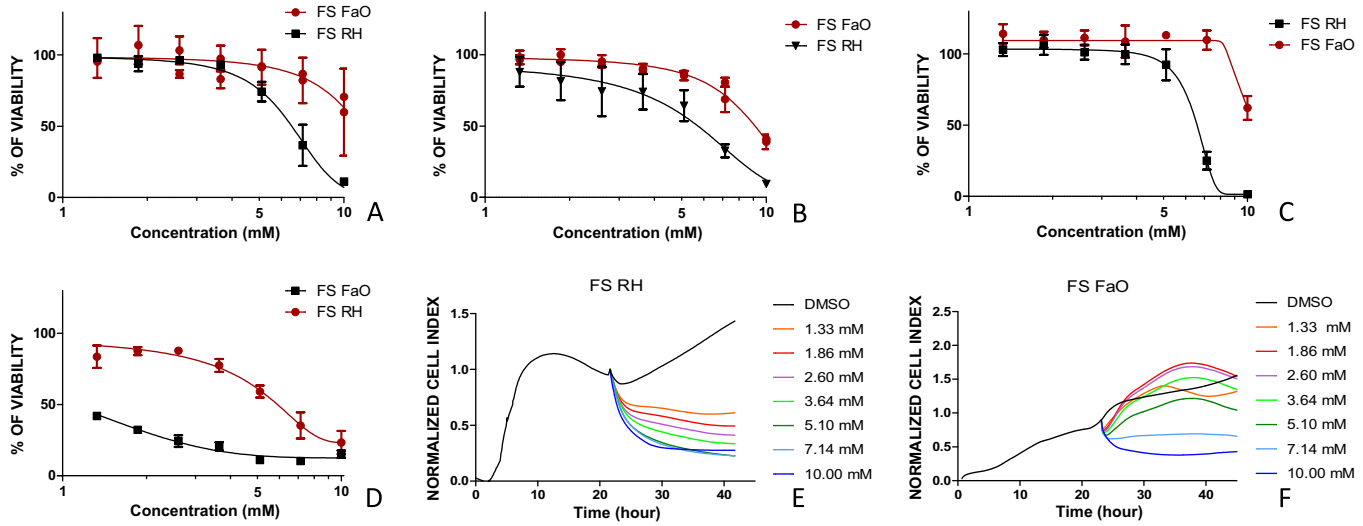

Fig. 8. Furosemide cytotoxicity monitoring of rat hepatocytes (RH) and FaO cell line. Cells were seeded onto 96-well plates and treated for 24 h with increasing concentrations of furosemide (FURO). Then, cell viability was assessed using MTT assay (A), NRU (B), ATP monitoring (C) and real-time impedance (D). (A–D) Results are presented as a percentage of viability over DMSO treatment and each value is the mean ± S.D. of three separate experiments. (E and F) Real-time impedance curves obtained from the xCELLigence system (Roche). Each curve was normalized just before compound addition on rat hepatocytes (E) or FaO cells (F) and represents an average of triplicate values.

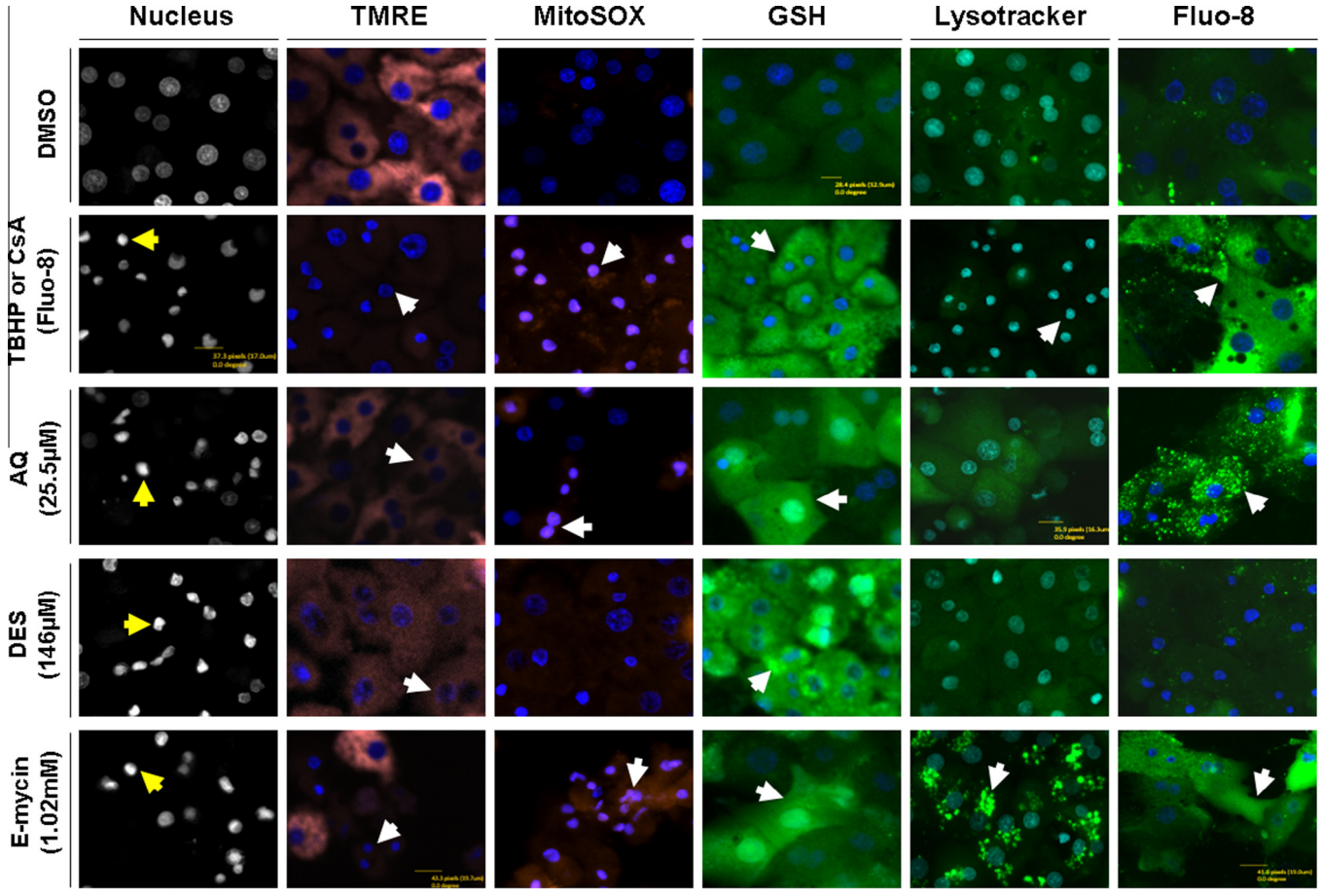

Fig. 9. Effects of several drugs on the main cellular functions of hepatic cells. Primary culture of rat hepatocytes were seeded onto 96-well plates and treated for 24 h with increasing concentrations of acetaminophen, retinoic acid, amodiaquine, carbamazepine, cyclophosphamide, diethylstilbestrol, erythromycin and furosemide. Cells were then stained with Hoechst 33342 and TMRE (30 min), MitoSOX (15 min), GSH (30 min), LysoTracker (45 min) or Fluo-8 (20 min). Spot intensity was detected with the ArrayScan^{XTI} and expressed as a ratio relative to the negative control DMSO. 500 µM of tert-butyl hydroperoxide (TBHP; 1 h of treatment) and 10 µM of cyclosporine A (CsA; 24 h of treatment) were used as a positive control. Amodiaquine – AQ (25.5 µM), diethylstilbestrol – DES (146 µM) and erythromycin – E-mycin (1.02 mM) conditions were chosen to illustrate the HCS imaging contribution.

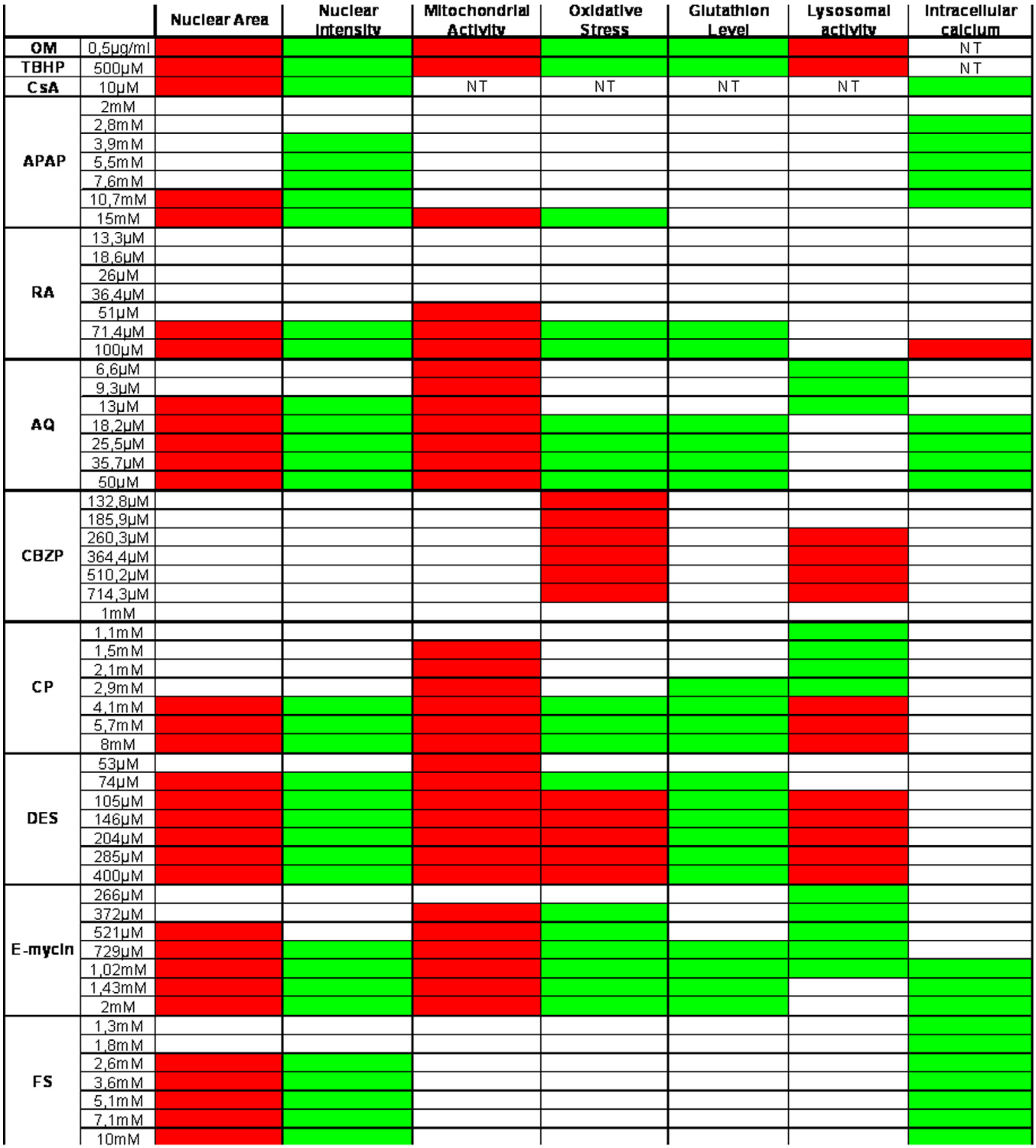

Fig. 10. Summary of the effects of drugs on main cellular functions of hepatic cells. Primary culture of rat hepatocytes were seeded onto 96-well plates and treated for 24 h with increasing concentrations of acetaminophen, retinoic acid, amodiaquine, carbamazepine, cyclophosphamide, diethylstilbestrol, erythromycin and furosemide. Cells were then stained with Hoechst 33342 and TMRE (30 min), MitoSOX (15 min), GSH (30 min), LysoTracker (45 min) or Fluo-8 (20 min). Spot intensity was detected with the ArrayScan^{XTI} and expressed as a ratio relative to the negative control DMSO. 500 µM of tert-butyl hydroperoxide (TBHP), 0.5 µg/ml oligomycin (OM) and 10 µM cyclosporine A (CsA) were used for 24 h as positive controls (except for TBHP, 1 h). Color legend: white means "no modulation", green "increase" and red "decrease". (For interpretation of the references to color in this figure legend, the reader is referred to the web version of this article.)

toxicity observed on rat hepatocytes could be linked to metabolic processes leading to drug bio-activation. The impedance curves (Fig. 7F) showed an increase in NCI for concentrations ranging from 0.4 to 1.5 mM, suggesting a possible cytomorphological effect in the absence of toxicity.

3.8. Furosemide hepatotoxicity is probably due to its impact on calcium storage

Furosemide (FURO) is a diuretic drug which improves kidney insufficiency. It is metabolized in the liver and has been associated

with hepatotoxicity (Qu et al., 2014). In our study, FURO cytotoxicity was low (IC_{50} = 4.66 mM with ATP monitoring, 4.92 mM with the NRU and 6.52 mM with the MTT test) yet the kinetics of the effect were rapid (Fig. 8A–C). Moreover, the impact of this drug on hepatocyte viability was dose-dependent, as suggested by the real-time cellular impedance data (Fig. 8D and E) which showed a much clearer biological response (IC_{50} = 1.4 mM). Using HCS technology (Fig. 10), we observed an alteration in nuclear integrity upon expositions in the range of 2.6–10 mM, while intracellular calcium increased (1.5-fold) at all concentrations tested (1.3–10 mM). We observed no additional modulation of cell functions.

FURO showed half the level of toxicity in FaO cells compared to in rat hepatocytes, suggesting that it is metabolized in the liver to produce toxic metabolites. Indeed, we noticed an IC_{50} of about 10 mM for the MTT, the NR and the ATP monitoring (Fig. 8A–C; Tables 2–4). While low doses (1.9–3.6 mM) increased the NCI (Fig. 8F), the highest concentrations (7.1 and 10 mM) provoked a significant decrease in the impedance value. However, at all concentrations tested, NCI displayed a quick and transitory decrease suggesting the possible occurrence of an early molecular and cellular event such as the modulation of calcium storage, as shown with HCS.

4. Discussion

Because liver is the main organ within which the detoxification of xenobiotics occurs, DILI represents the major cause of failure in drug development and the major reason for their withdrawal. The early detection of the hepatotoxic effects of drugs and chemicals to prevent such a huge economical loss through failure is crucial. Some *in vitro* cells cultures currently used to detect DILI are not always metabolically competent and therefore sensitive enough for use in drug assessment (Gerets et al., 2012). The same holds true for traditional cytotoxic assays (Miret et al., 2006). Indeed, the limited xenobiotic metabolizing potential of commonly-used indicator cell lines is one of the major disadvantages of *in vitro* methods. Due to their biochemical properties (binding to macromolecules, depleting the antioxidant cellular pool, etc.), reactive metabolites represent a leading cause of adverse drug reactions, which are not predicted accurately by current preclinical testing methodologies. Accounting for the metabolism process is therefore crucial for *in vitro* toxicological test development. The absence of such determinants of toxicity could give rise to falsely positive (lack of detoxification) or negative data (lack of bio-activation), as specified in the 2006 OECD report (see references part). For this reason, the visualization of xenobiotics metabolizing within hepatocytes is now considered as the best model for use in various areas of pharmaco-toxicological research.

In this context, we aimed to assess the potential applications of this model when coupled to real-time cellular impedance monitoring and high-content screening imaging. HCS technology has been proposed to solve such frequent toxicological drawbacks and be more predictive of human liver toxicity (Bale et al., 2014; Donato et al., 2012; Gerets et al., 2012; Kim et al., 2012; O'Brien et al., 2006; Persson et al., 2013; Porceddu et al., 2012; Seeland et al., 2013; Sirenko et al., 2014; Tolosa et al., 2012; Xu et al., 2008). Indeed, combining primary culture of human hepatocytes with this technology has already proven an interesting *in vitro* testing approach to identifying DILI positive drugs (Xu et al., 2008). Taking this further, we decided to compare conventional cytotoxic tests with two recent technologies: the real-time cellular impedance and the high-content imaging technology. To address the issue of hepatotoxicity linked to metabolic bio-activation, we compared eight drugs on two rat hepatic models: primary hepatocytes, known to be metabolically competent, and hepatoma cells, lacking most of the detoxification enzymes.

In primary culture of rat hepatocytes, our results from the MTT, the RN and the ATP uptake were comparable in terms of cell viability. However, MTT tended to under-estimate the mortality induced by the drugs tested. This can be explained by the drug-induced modulation of intracellular anion superoxide (decrease after carbamazepine and diethylstilbestrol expositions and increase for the other molecules) for all the compounds selected, except furosemide (and in a less obvious way acetaminophen). Anion superoxide is the predominant reactive oxygen species (ROS) linked to mitochondrial activity and is responsible for cellular damage (Dawson et al., 1993; Pessayre et al., 2004, 2012). The MTT test appeared inappropriate for investigating DILI which most often involved mitochondrial functioning (Labbe et al., 2008). Thus, among these three classical assays, the ATP and the NR uptake would appear to be the most relevant tests on this cell model.

In parallel, the NCI provided the dose-dependent effect of some drugs such as amodiaquine, retinoic acid, diethylstilbestrol, erythromycin and furosemide, while for others such results were not observed (cyclophosphamide, carbamazepine and acetaminophen). However, for methodological reasons that to date remain unclear, the rat hepatocytes model appears inappropriate for the study of cell viability with real-time cellular impedance. Indeed, the control DMSO alone increased the NCI, while for all the compounds tested and from the lowest concentrations, the NCI decreased 30–50%. Besides a lack of evidence in the literature for DMSO inducing such an effect, this increase in NCI observed in the control condition cannot be assigned to a proliferative effect since primary cultures of rat hepatocytes are blocked in G1 phase (Ichihara et al., 1982). It could however be associated with other cellular phenomena, such as resistance to spontaneous apoptosis, dedifferentiation, cell-junctions formation or extra-cellular matrix remodeling, which all happen during static hepatocyte culture (Bailly-Maitre et al., 2002; Fraczek et al., 2013; Martinez-Hernandez and Amenta, 1983; Weiner et al., 1996). In contrast with the increase induced by DMSO, all the drugs used in our study seemed to reduce the NCI making real-time cellular impedance monitoring unsuitable with this cell model. A similar observation has also been made by Atienzar's team (2013) who reported a low correlation of around 55% between classical cytotoxic assay and real-time cellular impedance using primary culture of human and rat hepatocytes. This holds true on human keratinocytes NHEK (Atienzar et al., 2011) and on primary neurons (Diemert et al., 2012), arguing against the use of primary cultures for impedance monitoring. Nevertheless, kinetics of effects and cell index curves could be considered as good indicators for cellular impacts of compounds on liver cells, especially on the HepG2 cell line already tested during our last investigations (Peyre et al., 2014). Moreover, impedance measurements in real-time condition constitute a unique tool to study the adaptative response of the cells to a chemical stress. Hence, in the present study, we observed very progressive kinetics of toxicity for retinoic acid in contrast to very fast kinetics for diethylstilbestrol, amodiaquine, furosemide and to a lesser extent erythromycin. This suggests a slower action for retinoic acid in comparison with the other compounds tested. Moreover, the NCI upon xenobiotic treatments is modulated by phenotypical modifications that could be related to biological perturbations. Despite of the difficulties of interpretation, the general curves obtained from impedance assay in primary cultured hepatocytes could be correlated to HCS results that provide a precise investigation at individual cells and their metabolic status. For instance, the dose-dependent decrease of NCI upon erythromycin treatment occurs in parallel with the formation of ROS (as quantified by MitoSOX™ Red assay). Moreover, amodiaquine, a prototypical pro-oxidant compound, increased the relative oxidative stress (as measured by MitoSOX™ Red assay) as well as GSH level (as quantified by ThiolTracker™ Violet) from 1.02 to 2 mM,

concentrations for which an important cytotoxicity is observed (as measured by NRU). However, we observed a transient increased in lysosomal activity for concentrations ranging from 266 μM to 1.02 mM (sub-toxic concentrations), that could be consistent with an adaptative response related to an increased autophagic process in response to chemical stress induced by amodiaquine. Hence, our results suggest that the early phenotypical modifications occurring after xenobiotics exposure could be detected by impedance measurements and further characterized by the HCS technology. Despite of the difficulties to use the primary cultures in impedance measurements, the overall curve obtained could be of interest to characterize the further adaptative response of cells upon chemical stress.

On FaO cells, the various evaluation methods of cell viability showed good correspondence. This first point to be made is that hepatic metabolism (missing in this hepatoma model) leads to molecular and cellular effects that modulate the detection of cytotoxicity by those tests which depend on these cellular functions. Secondly, the comparison between FaO cells and primary culture of rat hepatocytes provides interesting data. For example, while acetaminophen exposure showed no toxicity on FaO cells, we detected a toxicity of 10 mM in hepatocytes. This difference indicates that hepatotoxicity is dependent on bio-activation. The electrophilic metabolite N-acetylbenzoquinoneimine (NAPQI) is conventionally thought to provoke the hepatotoxic process. Indeed NAPQI is detoxified by GSH conjugation to form an acetaminophen-GSH conjugate. At high APAP concentration, total hepatic GSH is depleted, and as a result, the NAPQI covalently binds to proteins, forming acetaminophen-protein adducts (Mitchell et al., 1973). However, additional pathways could be involved in the detoxication processes involving Cytochrome P450 (CYP1A1, CYP1A2, CYP2A6, CYP2B1, CYP2E1, CYP3A4, CYP2D6 and CYP2A13), sulfotransferase or UDP-glucuronosyltransferases (Larson, 2007). Although much information has been published on APAP metabolism, the biochemical factors that determine hepatotoxicity outcome remain unclear. Hence, detoxication of APAP is complex and it has been proposed that besides CYPs activities, probably many factors contribute to processes leading to liver damage (Jemnitz et al., 2008; Patten et al., 1993; Thummel et al., 1993; Chen et al., 1998). Giving our results, we could suppose that depletion of GSH is not the only factor responsible of the cytotoxicity observed upon APAP exposure, suggesting another way of mechanism of toxicity than NAPQI (e.g. oxidative stress, mitochondrial permeability, apoptosis, etc.) as mentioned in the work of Jemnitz et al. (2008) and Masubuchi et al. (2005).

Another example is provided by the case of amodiaquine. Although the IC_{50} values are close in the two cell models, we noted a 2-fold difference with cellular impedance measurement, with faster kinetics on hepatocytes. This amplified toxicity on hepatocyte appears once again to be linked to bio-activation processes. Two other compounds exhibited a similar profile linked to biotransformation: erythromycin and furosemide. Indeed, these two drugs appeared more cytotoxic towards hepatocytes than to FaO cells. In addition to these four molecules showing different toxicity profiles depending on the model used, the four other compounds tested presented specific characteristics. Concerning diethylstilbestrol exposition, the hepatotoxicity was two to four times higher in FaO cells than in hepatocytes. In this case, the toxicity would therefore appear to not be linked to biotransformation, and metabolism could have a beneficial effect on direct DES toxicity. Interestingly and only based on IC_{50} comparison and cellular impedance kinetics, we concluded that cyclophosphamide was not significantly hepatotoxic and its biotransformation had no effects on non-mitotic cells. However, the HCS results showed that this compound alters the proper functioning of mitochondria and lysosomes at non-toxic doses, suggesting that this drug could be hepatotoxic under chronic conditions and may also be associated with DILI, as already shown (Abraham and Sugumar, 2008; Patel et al., 2009; Subramaniam et al., 2013). In the same way, HCS technology allowed us to better evaluate the effects of carbamazepine, which is non-toxic for both FaO cells and hepatocytes, yet it is able to downregulate the lysosomal activity, probably due to its anti-oxidant properties. These data are in concordance with those reported on mouse hepatocytes, where carbamazepine was found to reduce cell death and autophagy (Kim et al., 2013). Concerning retinoic acid, toxicity would not appear to depend on bio-activation since we observed similar IC_{50} for the two models and whatever the test used.

Finally, high content screening provided us with an overview on the main cellular dysfunctions induced by the tested drugs. First, nuclear integrity appears to be a good indicator as regards cell death (Earnshaw, 1995; Loo and Rillema, 1998; Toné et al., 2007). Here we noted that after toxic exposure, nuclear area was inversely proportional to nuclear intensity, indicating that drug-induced toxicity leads to a decrease in nuclear area and to an increase in its intensity, as detected via Hoechst 33342. Only acetaminophen appeared capable of significantly modifying the nuclear intensity without changing the nuclear area. Among all the numerous chemicals tested in our laboratory, this is the first time we have observed such an event. We hypothesize a possible link between this process and an increase in intracellular calcium however the involved mechanism requires further investigation. We did identify a two-step event occurring with acetaminophen, the first linked to calcium flux and the second to oxidative stress and downregulation of mitochondrial activity, as already suggested (Bajt et al., 2004, 2011; Jaeschke et al., 2012). Using HCS, we also demonstrated, as already suggested by many studies, that retinoic acid (Ribeiro et al., 2013; Tan et al., 2008), amodiaquine (Tafazoli and O'Brien, 2009), cyclophosphamide (Kumari and Setty, 2012; Tripathi and Jena, 2010), diethylstilbestrol (Kipp and Ramirez, 2001; Li et al., 2011) and erythromycin (Anandatheerthavarada et al., 1999; Lu et al., 2014) induced oxidative stress and mitochondrial dysfunction. Interestingly, coupling information from HCS and xCELLigence allowed us to conclude that amodiaquine first acts on mitochondria before inducing ROS production. Indeed, we first detected a decrease in mitochondrial potential with a parallel increase in lysosomal activity. The second event was an increase in GSH that occurred in parallel to an increased detection of ROS. This observation is in accordance with the biphasic impedance profile which first shows an increase of the cell index, before decreasing under the DMSO control. Another interesting observation made using HCS was the case of cyclophosphamide. At non-toxic concentrations, this drug (when bioactivated) induced an increase in lysosomal and decrease in mitochondrial activity before acting as a pro-oxidant compound at the highest doses. Such perturbations have already been reported in rat kidney (Abraham and Isaac, 2011) and in liver (Lushnikova et al., 2011). As concerns erythromycin, an antibiotic drug able to induce hepatitis, hepatic dysfunction, jaundice and necrosis of hepatocytes at high dose (Pessayre et al., 1985), our study underlined not only its pro-oxidant properties leading to cytotoxicity but also it leading to an increase of lysosomal activity, as already shown (Cox et al., 1988). Perturbation of lysosomal function has been correlated with phospholipidosis (Atienzar et al., 2007; Gerbaux et al., 1996) and then hepatic injury (Anthérieu et al., 2012), making crucial an early detection of such an event for drug development.

These various examples illustrate the huge potential of this combined toxicological approach, for the early identification of bio-activation processes which represent a leading cause of adverse drug reactions often overlooked by current preclinical

testing methodology. This mechanistic-based approach is explanatory, sensitive, reproducible, and more accurately predictive of the toxic response in vertebrates, and is suitable for coupling with for example *in silico* methods for reducing, refining and replacing the use of laboratory animals.

To conclude, the correlation between the outcomes from different methods used in our study to evaluate cellular viability depended on the biological model used. For an objective assessment and to increase the sensitivity of tests, we believe it crucial to exploit multiparametric tests such as HCS. Globally, the neutral red uptake appeared a well-adapted test for all the models used. MTT and ATP monitoring on the other hand should to be used with caution, particularly for cells sensitive to oxidative stress or for primary cultures respectively. Although our data indicate cellular impedance as the most sensitive test, we propose using this method as a secondary cytotoxic evaluation tool to complement standard assays. The real-time impedance curves are good indicators of dose dependence, kinetics of action and consequently of hepatic bio-activation. When no significant differences were found between the IC_{50}, the kinetics were faster on freshly isolated hepatocytes suggesting the involvement of bio-activation in toxicity. The impedance curves also constitute molecular profiles that provide a useful guide in the study of mechanisms of action. As such real-time cellular impedance might be considered as a useful tool in "behavioral cellular biology". However, this innovative technology must be employed in preference with cell lines and not, or at least with caution, with primary cultures.

Funding

This work was funded by the French Ministry of Ecology (as part of the ACTIVISME project), by the "Conseil Général des Alpes Maritimes" (as part of the HCSTOX project) and by Galderma R&D.

Conflict of Interest

The authors declare having no conflicts of interest.

Transparency Document

The Transparency document associated with this article can be found in the online version.

Acknowledgements

The authors wish to thank Roche for their help using the real-time cellular impedance technology (xCELLigence®), Galderma R&D (Sophia Antipolis) for their financial support, and Delphine Lemoine for her technical assistance.

Appendix A. Supplementary material

Supplementary data associated with this article can be found, in the online version, at http://dx.doi.org/10.1016/j.tiv.2015.07.024.

References

Abraham, P., Isaac, B., 2011. Ultrastructural changes in the rat kidney after single dose of cyclophosphamide – possible roles for peroxisome proliferation and lysosomal dysfunction in cyclophosphamide-induced renal damage. Hum. Exp. Toxicol. 30 (12), 1924–1930. http://dx.doi.org/10.1177/0960327111402240.

Abraham, P., Sugumar, E., 2008. Increased glutathione levels and activity of PON1 (phenyl acetate esterase) in the liver of rats after a single dose of cyclophosphamide: a defense mechanism? Exp. Toxicol. Pathol. 59 (5), 301–306. http://dx.doi.org/10.1016/j.etp.2007.06.006.

Anandatheerthavarada, H.K., Vijayasarathy, C., Bhagwat, S.V., Biswas, G., Mullick, J., Avadhani, N.G., 1999. Physiological role of the N-terminal processed P4501A1 targeted to mitochondria in erythromycin metabolism and reversal of erythromycin-mediated inhibition of mitochondrial protein synthesis. J. Biol. Chem. 274 (10), 6617–6625.

Ansede, J.H., Smith, W.R., Perry, C.H., St Claire, R.L., Brouwer, K.R., 2010. An in vitro assay to assess transporter-based cholestatic hepatotoxicity using sandwich-cultured rat hepatocytes. Drug Metab. Dispos. 38 (2), 276–280. http://dx.doi.org/10.1124/dmd.109.028407.

Anthérieu, S., Chesné, C., Li, R., Guguen-Guillouzo, C., Guillouzo, A., 2012. Optimization of the HepaRG cell model for drug metabolism and toxicity studies. Toxicol. in Vitro 26 (8), 1278–1285. http://dx.doi.org/10.1016/j.tiv.2012.05.008.

Atienzar, F.A., Tilmant, K., Gerets, H.H., Toussaint, G., Speeckaert, S., Hanon, E., Depelchin, O., Dhalluin, S., 2011. The use of real-time cell analyzer technology in drug discovery: defining optimal cell culture conditions and assay reproducibility with different adherent cellular models. J. Biomol. Screen. 16 (6), 575–587. http://dx.doi.org/10.1177/1087057111402825.

Atienzar, F., Gerets, H., Dufrane, S., Tilmant, K., Cornet, M., Dhalluin, S., Ruty, B., Rose, G., Canning, M., 2007. Determination of phospholipidosis potential based on gene expression analysis in HepG2 cells. Toxicol. Sci. 96 (1), 101–114. http://dx.doi.org/10.1093/toxsci/kfl184.

Bailly-Maitre, B., de Sousa, G., Zucchini, N., Gugenheim, J., Boulukos, K.E., Rahmani, R., 2002. Spontaneous apoptosis in primary cultures of human and rat hepatocytes: molecular mechanisms and regulation by dexamethasone. Cell Death Differ. 9 (9), 945–955. http://dx.doi.org/10.1038/sj/cdd/4401043.

Bajt, M.L., Knight, T.R., Lemasters, J.J., Jaeschke, H., 2004. Acetaminophen-induced oxidant stress and cell injury in cultured mouse hepatocytes: protection by N-acetyl cysteine. Toxicol. Sci. 80 (2), 343–349. http://dx.doi.org/10.1093/toxsci/kfh151.

Bajt, M.L., Ramachandran, A., Yan, H.M., Lebofsky, M., Farhood, A., Lemasters, J.J., Jaeschke, H., 2011. Apoptosis-inducing factor modulates mitochondrial oxidant stress in acetaminophen hepatotoxicity. Toxicol. Sci. 122 (2), 598–605. http://dx.doi.org/10.1093/toxsci/kfr116.

Bale, S.S., Vernetti, L., Senutovitch, N., Jindal, R., Hegde, M., Gough, A., McCarty, W.J., Bakan, A., Bhushan, A., Shun, T.Y., Golberg, I., Debiasio, R., Usta, B.O., Taylor, D.L., Yarmush, M.L., 2014. In vitro platforms for evaluating liver toxicity. Exp. Biol. Med. (Maywood). http://dx.doi.org/10.1177/1535370214531872.

Berry, M.N., Friend, D.S., 1969. High-yield preparation of isolated rat liver parenchymal cells: a biochemical and fine structural study. J. Cell Biol. 43 (3), 506–520.

Biour, M., Ben Salem, C., Chazouillères, O., Grangé, J.D., Serfaty, L., Poupon, R., 2004. Drug-induced liver injury; fourteenth updated edition of the bibliographic database of liver injuries and related drugs. Gastroenterol. Clin. Biol. 28 (8–9), 720–759.

Chen, W., Koenigs, L.L., Thompson, S.J., Peter, R.M., Rettie, A.E., Trager, W.F., Nelson, S.D., 1998. Oxidation of acetaminophen to its toxic quinone imine and nontoxic catechol metabolites by baculovirus-expressed and purified human cytochromes P450 2E1 and 2A6. Chem. Res. Toxicol. 11 (4), 295–301.

Coecke, S., Ahr, H., Blaauboer, B.J., Bremer, S., Casati, S., Castell, J., Combes, R., Corvi, R., Crespi, C.L., Cunningham, M.L., Elaut, G., Eletti, B., Freidig, A., Gennari, A., Ghersi-Egea, J.F., Guillouzo, A., Hartung, T., Hoet, P., Ingelman-Sundberg, M., Munn, S., Janssens, W., Ladstetter, B., Leahy, D., Long, A., Meneguz, A., Monshouwer, M., Morath, S., Nagelkerke, F., Pelkonen, O., Ponti, J., Prieto, P., Richert, L., Sabbioni, E., Schaack, B., Steiling, W., Testai, E., Vericat, J.A., Worth, A., 2006. Metabolism: a bottleneck in in vitro toxicological test development. The report and recommendations of ECVAM workshop 54. Altern. Lab. Anim. 34 (1), 49–84.

Cox, J.W., Ulrich, R.G., Larson, P.G., Cramer, C.T., 1988. Acute hepatocellular effects of erythromycin, gentamicin, and trospectomycin in the perfused rat liver: lack of correlation between lamellar body induction potency and cytotoxicity. Pharmacol. Toxicol. 62 (5), 337–343.

Crépet, A., Héraud, F., Béchaux, C., Gouze, M.E., Pierlot, S., Fastier, A., Leblanc, J.C.h., Le Hégarat, L., Takakura, N., Fessard, V., Tressou, J., Maximilien, R., de Sousa, G., Nawaz, A., Zucchini-Pascal, N., Rahmani, R., Audebert, M., Graillot, V., Cravedi, J.P., 2013. The PERICLES research program: an integrated approach to characterize the combined effects of mixtures of pesticide residues to which the French population is exposed. Toxicology 313 (2–3), 83–93. http://dx.doi.org/10.1016/j.tox.2013.04.005.

Dawson, T.L., Gores, G.J., Nieminen, A.L., Herman, B., Lemasters, J.J., 1993. Mitochondria as a source of reactive oxygen species during reductive stress in rat hepatocytes. Am. J. Physiol. 264 (4 Pt 1), C961–C967.

de Sousa, G., Dou, M., Barbe, D., Lacarelle, B., Placidi, M., Rahmani, R., 1991. Freshly isolated or cryopreserved human hepatocytes in primary culture: influence of drug metabolism on hepatotoxicity. Toxicol. in Vitro 5 (5–6), 483–486.

Diemert, S., Dolga, A.M., Tobaben, S., Grohm, J., Pfeifer, S., Oexler, E., Culmsee, C., 2012. Impedance measurement for real time detection of neuronal cell death. J. Neurosci. Meth. 203 (1), 69–77. http://dx.doi.org/10.1016/j.jneumeth.2011.09.012.

Donato, M.T., Tolosa, L., Jiménez, N., Castell, J.V., Gómez-Lechón, M.J., 2012. High-content imaging technology for the evaluation of drug-induced steatosis using a multiparametric cell-based assay. J. Biomol. Screen. 17 (3), 394–400. http://dx.doi.org/10.1177/1087057111427586.

Earnshaw, W.C., 1995. Nuclear changes in apoptosis. Curr. Opin. Cell Biol. 7 (3), 337–343.

Fautrel, A., Chesné, C., Guillouzo, A., de Sousa, G., Placidi, M., Rahmani, R., Braut, F., Pichon, J., Hoellinger, H., Vintézou, P., Diarte, I., Melcion, C., Cordier, A., Lorenzon, G., Benicourt, M., Vannier, B., Fournex, R., Peloux, A.F., Bichet, N., Gouy, D., Cano, J.P., Lounes, R., 1991. A multicentre study of acute in vitro cytotoxicity in rat liver cells. Toxicol. in Vitro 5 (5–6), 543–547.

Fraczek, J., Bolleyn, J., Vanhaecke, T., Rogiers, V., Vinken, M., 2013. Primary hepatocyte cultures for pharmaco-toxicological studies: at the busy crossroad of various anti-dedifferentiation strategies. Arch. Toxicol. 87 (4), 577–610. http://dx.doi.org/10.1007/s00204-012-0983-3.

Gerbaux, C., Van Bambeke, F., Montenez, J.P., Piret, J., Morlighem, G., Tulkens, P.M., 1996. Hyperactivity of cathepsin B and other lysosomal enzymes in fibroblasts exposed to azithromycin, a dicationic macrolide antibiotic with exceptional tissue accumulation. FEBS Lett. 394 (3), 307–310.

Gerets, H.H., Tilmant, K., Gerin, B., Chanteux, H., Depelchin, B.O., Dhalluin, S., Atienzar, F.A., 2012. Characterization of primary human hepatocytes, HepG2 cells, and HepaRG cells at the mRNA level and CYP activity in response to inducers and their predictivity for the detection of human hepatotoxins. Cell Biol. Toxicol. 28 (2), 69–87. http://dx.doi.org/10.1007/s10565-011-9208-4.

Guillouzo, A., Corlu, A., Aninat, C., Glaise, D., Morel, F., Guguen-Guillouzo, C., 2007. The human hepatoma HepaRG cells: a highly differentiated model for studies of liver metabolism and toxicity of xenobiotics. Chem. Biol. Interact. 168 (1), 66–73. http://dx.doi.org/10.1016/j.cbi.2006.12.003.

Gómez-Lechón, M.J., Castell, J.V., Donato, M.T., 2010. The use of hepatocytes to investigate drug toxicity. Meth. Mol. Biol. 640, 389–415. http://dx.doi.org/10.1007/978-1-60761-688-7_21.

Hart, S.N., Li, Y., Nakamoto, K., Subileau, E.A., Steen, D., Zhong, X.B., 2010. A comparison of whole genome gene expression profiles of HepaRG cells and HepG2 cells to primary human hepatocytes and human liver tissues. Drug Metab. Dispos. 38 (6), 988–994. http://dx.doi.org/10.1124/dmd.109.031831.

Higuchi, S., Yano, A., Takai, S., Tsuneyama, K., Fukami, T., Nakajima, M., Yokoi, T., 2012. Metabolic activation and inflammation reactions involved in carbamazepine-induced liver injury. Toxicol. Sci. 130 (1), 4–16. http://dx.doi.org/10.1093/toxsci/kfs222.

Hill, A., Mesens, N., Steemans, M., Xu, J.J., Aleo, M.D., 2012. Comparisons between in vitro whole cell imaging and in vivo zebrafish-based approaches for identifying potential human hepatotoxicants earlier in pharmaceutical development. Drug Metab. Rev. 44 (1), 127–140. http://dx.doi.org/10.3109/03602532.2011.645578.

Ichihara, A., Nakamura, T., Tanaka, K., 1982. Use of hepatocytes in primary culture for biochemical studies on liver functions. Mol. Cell. Biochem. 43 (3), 145–160.

Jaeschke, H., McGill, M.R., Ramachandran, A., 2012. Oxidant stress, mitochondria, and cell death mechanisms in drug-induced liver injury: lessons learned from acetaminophen hepatotoxicity. Drug Metab. Rev. 44 (1), 88–106. http://dx.doi.org/10.3109/03602532.2011.602688.

Jemnitz, K., Veres, Z., Monostory, K., Kóbori, L., Vereczkey, L., 2008. Interspecies differences in acetaminophen sensitivity of human, rat, and mouse primary hepatocytes. Toxicol. in Vitro 22 (4), 961–967. http://dx.doi.org/10.1016/j.tiv.2008.02.001.

Ke, N., Wang, X., Xu, X., Abassi, Y.A., 2011. The xCELLigence system for real-time and label-free monitoring of cell viability. Meth. Mol. Biol. 740, 33–43. http://dx.doi.org/10.1007/978-1-61779-108-6_6.

Kim, J.A., Han, E., Eun, C.J., Tak, Y.K., Song, J.M., 2012. Real-time concurrent monitoring of apoptosis, cytosolic calcium, and mitochondria permeability transition for hypermulticolor high-content screening of drug-induced mitochondrial dysfunction-mediated hepatotoxicity. Toxicol. Lett. 214 (2), 175–181. http://dx.doi.org/10.1016/j.toxlet.2012.08.027.

Kim, J.S., Wang, J.H., Biel, T.G., Kim, D.S., Flores-Toro, J.A., Vijayvargiya, R., Zendejas, I., Behrns, K.E., 2013. Carbamazepine suppresses calpain-mediated autophagy impairment after ischemia/reperfusion in mouse livers. Toxicol. Appl. Pharmacol. 273 (3), 600–610. http://dx.doi.org/10.1016/j.taap.2013.10.006.

Kipp, J.L., Ramirez, V.D., 2001. Effect of estradiol, diethylstilbestrol, and resveratrol on F0F1-ATPase activity from mitochondrial preparations of rat heart, liver, and brain. Endocrine 15 (2), 165–175. http://dx.doi.org/10.1385/ENDO:15:2:165.

Kumari, K.K., Setty, O.H., 2012. Protective effect of *Phyllanthus fraternus* against mitochondrial dysfunction induced by co-administration of cisplatin and cyclophosphamide. J. Bioenerg. Biomembr. 44 (1), 179–188. http://dx.doi.org/10.1007/s10863-012-9423-6.

Labbe, G., Pessayre, D., Fromenty, B., 2008. Drug-induced liver injury through mitochondrial dysfunction: mechanisms and detection during preclinical safety studies. Fundam. Clin. Pharmacol. 22 (4), 335–353. http://dx.doi.org/10.1111/j.1472-8206.2008.00608.x.

Lam, J.L., Okochi, H., Huang, Y., Benet, L.Z., 2006. In vitro and in vivo correlation of hepatic transporter effects on erythromycin metabolism: characterizing the importance of transporter-enzyme interplay. Drug Metab. Dispos. 34 (8), 1336–1344. http://dx.doi.org/10.1124/dmd.106.009258.

Larrey, D., 2009. Hepatotoxicity of drugs and chemicals. Gastroenterol. Clin. Biol. 33 (12), 1136–1146. http://dx.doi.org/10.1016/j.gcb.2009.10.003.

Larson, A.M., 2007. Acetaminophen hepatotoxicity. Clin. Liver Dis. 11 (3), 525–548.

Lecluyse, E.L., Alexandre, E., 2010. Isolation and culture of primary hepatocytes from resected human liver tissue. Meth. Mol. Biol. 640, 57–82. http://dx.doi.org/10.1007/978-1-60761-688-7_3.

Li, Y., Okumura, K., Nomura, S., Maeda, N., Miyasho, T., Yokota, H., 2011. Oxidatively damaged proteins in the early stage of testicular toxicities in male rats by orally administered with a synthetic oestrogen, diethylstilbestrol. Reprod. Toxicol. 31 (1), 26–34. http://dx.doi.org/10.1016/j.reprotox.2010.09.007.

Limame, R., Wouters, A., Pauwels, B., Fransen, E., Peeters, M., Lardon, F., De Wever, O., Pauwels, P., 2012. Comparative analysis of dynamic cell viability, migration and invasion assessments by novel real-time technology and classic endpoint assays. PLoS One 7 (10), e46536. http://dx.doi.org/10.1371/journal.pone.0046536.

Loo, D.T., Rillema, J.R., 1998. Measurement of cell death. Meth. Cell Biol. 57, 251–264.

Lu, X., Tian, Y., Lian, X., Jin, Y., Jin, T., Zhao, Q., Hu, B., Shen, X., Fan, X., 2014. Integrated systems toxicology approaches identified the possible involvement of ABC transporters pathway in erythromycin estolate-induced liver injury in rat. Food Chem. Toxicol. 65, 343–355. http://dx.doi.org/10.1016/j.fct.2013.12.050.

Lushnikova, E.L., Molodykh, O.P., Nepomnyashchikh, L.M., Bakulina, A.A., Sorokina, Y.A., 2011. Ultrastructural picture of cyclophosphamide-induced damage to the liver. Bull. Exp. Biol. Med. 151 (6), 751–756.

Maier, P., 1988. Development of in vitro toxicity tests with cultures of freshly isolated rat hepatocytes. Experientia 44 (10), 807–817.

Marchandeau, J.P., Labbe, G., 2011. Evaluation of mitochondrial respiration in cultured rat hepatocytes. Meth. Mol. Biol. 691, 243–253. http://dx.doi.org/10.1007/978-1-60761-849-2_14.

Martinez-Hernandez, A., Amenta, P.S., 1993. The hepatic extracellular matrix. I. Components and distribution in normal liver. Virchows Arch. A Pathol. Anat. Histopathol. 423 (1), 1–11.

Martinez-Serra, J., Gutierrez, A., Muñoz-Capó, S., Navarro-Palou, M., Ros, T., Amat, J.C., Lopez, B., Marcus, T.F., Fueyo, L., Suquia, A.G., Gines, J., Rubio, F., Ramos, R., Besalduch, J., 2014. XCELLigence system for real-time label-free monitoring of growth and viability of cell lines from hematological malignancies. Onco Targets Ther. 7, 985–994. http://dx.doi.org/10.2147/OTT.S62887.

Masubuchi, Y., Suda, C., Horie, T., 2005. Involvement of mitochondrial permeability transition in acetaminophen-induced liver injury in mice. J. Hepatol. 42 (1), 110–116.

McGill, M.R., Jaeschke, H., 2013. Metabolism and disposition of acetaminophen: recent advances in relation to hepatotoxicity and diagnosis. Pharm. Res. 30 (9), 2174–2187. http://dx.doi.org/10.1007/s11095-013-1007-6.

Miret, S., De Groene, E.M., Klaffke, W., 2006. Comparison of in vitro assays of cellular toxicity in the human hepatic cell line HepG2. J. Biomol. Screen. 11 (2), 184–193. http://dx.doi.org/10.1177/1087057105283787.

Mitchell, J.R., Jollow, D.J., Potter, W.Z., Gillette, J.R., Brodie, B.B., 1973. Acetaminophen-induced hepatic necrosis. IV. Protective role of glutathione. J. Pharmacol. Exp. Ther. 187 (1), 211–217.

Nawaz, A., Razpotnik, A., Rouimi, P., de Sousa, G., Cravedi, J.P., Rahmani, R., 2014. Cellular impact of combinations of endosulfan, atrazine, and chlorpyrifos on human primary hepatocytes and HepaRG cells after short and chronic exposures. Cell Biol. Toxicol. 30 (1), 17–29. http://dx.doi.org/10.1007/s10565-013-9266-x.

O'Brien, P.J., Irwin, W., Diaz, D., Howard-Cofield, E., Krejsa, C.M., Slaughter, M.R., Gao, B., Kaludercic, N., Angeline, A., Bernardi, P., Brain, P., Hougham, C., 2006. High concordance of drug-induced human hepatotoxicity with in vitro cytotoxicity measured in a novel cell-based model using high content screening. Arch. Toxicol. 80 (9), 580–604.

Oesch, F., Diener, B., 1995. Cell systems for use in studies on the relationship between foreign compound metabolism and toxicity. Pharmacol. Toxicol. 76 (5), 325–327.

Ostapowicz, G., Fontana, R.J., Schiødt, F.V., Larson, A., Davern, T.J., Han, S.H., McCashland, T.M., Shakil, A.O., Hay, J.E., Hynan, L., Crippin, J.S., Blei, A.T., Samuel, G., Reisch, J., Lee, W.M.U.S. Acute Liver Failure Study Group, 2002. Results of a prospective study of acute liver failure at 17 tertiary care centers in the United States. Ann. Intern. Med. 137 (12), 947–954.

Patel, A., Patel, S., Jalandhara, P., Thakor, P., 2009. Cyclophosphamide therapy in granulomatous hepatitis: cure or culprit? Am. J. Ther. 16 (4), 367–370. http://dx.doi.org/10.1097/MJT.0b013e31818a88f0.

Patten, C.J., Thomas, P.E., Guy, R.L., Lee, M., Gonzalez, F.J., Guengerich, F.P., Yang, C.S., 1993. Cytochrome P450 enzymes involved in acetaminophen activation by rat and human liver microsomes and their kinetics. Chem. Res. Toxicol. 6 (4), 511–518.

Persson, M., Løye, A.F., Mow, T., Hornberg, J.J., 2013. A high content screening assay to predict human drug-induced liver injury during drug discovery. J. Pharmacol. Toxicol. Meth. 68 (3), 302–313. http://dx.doi.org/10.1016/j.vascn.2013.08.001.

Pessayre, D., Fromenty, B., Berson, A., Robin, M.A., Lettéron, P., Moreau, R., Mansouri, A., 2012. Central role of mitochondria in drug-induced liver injury. Drug Metab. Rev. 44 (1), 34–87. http://dx.doi.org/10.3109/03602532.2011.604086.

Pessayre, D., Fromenty, B., Mansouri, A., 2004. Mitochondrial injury in steatohepatitis. Eur. J. Gastroenterol. Hepatol. 16 (11), 1095–1105.

Pessayre, D., Larrey, D., Funck-Brentano, C., Benhamou, J.P., 1985. Drug interactions and hepatitis produced by some macrolide antibiotics. J. Antimicrob. Chemother. 16 (Suppl. A), 181–194.

Peyre, L., Zucchini-Pascal, N., de Sousa, G., Luzy, A.P., Rahmani, R., 2014. Potential involvement of chemicals in liver cancer progression: an alternative toxicological approach combining biomarkers and innovative technologies. Toxicol. in Vitro 28 (8), 1507–1520.

Pirmohamed, M., Kitteringham, N.R., Guenthner, T.M., Breckenridge, A.M., Park, B.K., 1992. An investigation of the formation of cytotoxic, protein-reactive and stable metabolites from carbamazepine in vitro. Biochem. Pharmacol. 43 (8), 1675–1682.

Ponsoda, X., Donato, M.T., Perez-Cataldo, G., Gómez-Lechón, M.J., Castell, J.V., 2004. Drug metabolism by cultured human hepatocytes: how far are we from the in vivo reality? Altern. Lab. Anim. 32 (2), 101–110.

Ponsoda, X., Jover, R., Núñez, C., Royo, M., Castell, J.V., Gómez-Lechón, M.J., 1995. Evaluation of the cytotoxicity of 10 chemicals in human and rat hepatocytes and in cell lines: correlation between in vitro data and human lethal concentration. Toxicol. in Vitro 9 (6), 959–966.

Porceddu, M., Buron, N., Roussel, C., Labbe, G., Fromenty, B., Borgne-Sanchez, A., 2012. Prediction of liver injury induced by chemicals in human with a multiparametric assay on isolated mouse liver mitochondria. Toxicol. Sci. 129 (2), 332–345. http://dx.doi.org/10.1093/toxsci/kfs197.

Prot, J.M., Leclerc, E., 2012. The current status of alternatives to animal testing and predictive toxicology methods using liver microfluidic biochips. Ann. Biomed. Eng. 40 (6), 1228–1243. http://dx.doi.org/10.1007/s10439-011-0480-5.

Qu, Q., Liu, J., Zhou, H.H., Klaassen, C.D., 2014. Nrf2 protects against furosemide-induced hepatotoxicity. Toxicology 324, 35–42. http://dx.doi.org/10.1016/j.tox.2014.02.008.

Ribeiro, M.P., Santos, A.E., Santos, M.S., Custódio, J.B., 2013. Effects of all-trans-retinoic acid on the permeability transition and bioenergetic functions of rat liver mitochondria in combination with endoxifen. Life Sci. 93 (2–3), 96–107. http://dx.doi.org/10.1016/j.lfs.2013.05.027.

Rodrigues, R.M., Bouhifd, M., Bories, G., Sacco, M.G., Gribaldo, L., Fabbri, M., Coecke, S., Whelan, M.P., 2013. Assessment of an automated in vitro basal cytotoxicity test system based on metabolically-competent cells. Toxicol. in Vitro 27 (2), 760–767. http://dx.doi.org/10.1016/j.tiv.2012.12.004.

Seeland, S., Török, M., Kettiger, H., Treiber, A., Hafner, M., Huwyler, J., 2013. A cell-based, multiparametric sensor approach characterises drug-induced cytotoxicity in human liver HepG2 cells. Toxicol. in Vitro 27 (3), 1109–1120. http://dx.doi.org/10.1016/j.tiv.2013.02.001.

Shmarakov, I.O., Borschovetska, V.L., Marchenko, M.M., Blaner, W.S., 2014. Retinoids modulate thioacetamide-induced acute hepatotoxicity. Toxicol. Sci. 139 (2), 284–292. http://dx.doi.org/10.1093/toxsci/kfu045.

Shull, L.R., Kirsch, D.G., Lohse, C.L., Wisniewski, J.A., 1987. Application of isolated hepatocytes to studies of drug metabolism in large food animals. Xenobiotica 17 (3), 345–363. http://dx.doi.org/10.3109/00498258709043944.

Sirenko, O., Hesley, J., Rusyn, I., Cromwell, E.F., 2014. High-content assays for hepatotoxicity using induced pluripotent stem cell-derived cells. Assay Drug Dev. Technol. 12 (1), 43–54. http://dx.doi.org/10.1089/adt.2013.520.

Subramaniam, S.R., Cader, R.A., Mohd, R., Yen, K.W., Ghafor, H.A., 2013. Low-dose cyclophosphamide-induced acute hepatotoxicity. Am. J. Case Rep. 14, 345–349. http://dx.doi.org/10.12659/AJCR.889401.

Suzuki, A., Andrade, R.J., Bjornsson, E., Lucena, M.I., Lee, W.M., Yuen, N.A., Hunt, C.M., Freston, J.W., 2010. Drugs associated with hepatotoxicity and their reporting frequency of liver adverse events in VigiBase: unified list based on international collaborative work. Drug Saf. 33 (6), 503–522. http://dx.doi.org/10.2165/11535340-000000000-00000.

Suzuki, H., Inoue, T., Matsushita, T., Kobayashi, K., Horii, I., Hirabayashi, Y., 2008. In vitro gene expression analysis of hepatotoxic drugs in rat primary hepatocytes. J. Appl. Toxicol. 28 (2), 227–236. http://dx.doi.org/10.1002/jat.1328.

Tafazoli, S., O'Brien, P.J., 2009. Amodiaquine-induced oxidative stress in a hepatocyte inflammation model. Toxicology 256 (1–2), 101–109. http://dx.doi.org/10.1016/j.tox.2008.11.006.

Tan, K.P., Kosuge, K., Yang, M., Ito, S., 2008. NRF2 as a determinant of cellular resistance in retinoic acid cytotoxicity. Free Radic. Biol. Med. 45 (12), 1663–1673. http://dx.doi.org/10.1016/j.freeradbiomed.2008.09.010.

Thummel, K.E., Lee, C.A., Kunze, K.L., Nelson, S.D., Slattery, J.T., 1993. Oxidation of acetaminophen to N-acetyl-p-aminobenzoquinone imine by human CYP3A4. Biochem. Pharmacol. 45 (8), 1563–1569.

Tolosa, L., Pinto, S., Donato, M.T., Lahoz, A., Castell, J.V., O'Connor, J.E., Gómez-Lechón, M.J., 2012. Development of a multiparametric cell-based protocol to screen and classify the hepatotoxicity potential of drugs. Toxicol. Sci. 127 (1), 187–198. http://dx.doi.org/10.1093/toxsci/kfs083.

Toné, S., Sugimoto, K., Tanda, K., Suda, T., Uehira, K., Kanouchi, H., Samejima, K., Minatogawa, Y., Earnshaw, W.C., 2007. Three distinct stages of apoptotic nuclear condensation revealed by time-lapse imaging, biochemical and electron microscopy analysis of cell-free apoptosis. Exp. Cell Res. 313 (16), 3635–3644. http://dx.doi.org/10.1016/j.yexcr.2007.06.018.

Tripathi, D.N., Jena, G.B., 2010. Astaxanthin intervention ameliorates cyclophosphamide-induced oxidative stress, DNA damage and early hepatocarcinogenesis in rat: role of Nrf2, p53, p38 and phase-II enzymes. Mutat. Res. 696 (1), 69–80. http://dx.doi.org/10.1016/j.mrgentox.2009.12.014.

Vega, A., Baptissart, M., Martinot, E., Saru, J.P., Baron, S., Schoonjans, K., Volle, D.H., 2014. Hepatotoxicity induced by neonatal exposure to diethylstilbestrol is maintained throughout adulthood via the nuclear receptor SHP. Exp. Opin. Ther. Targets 18 (12), 1367–1376. http://dx.doi.org/10.1517/14728222.2014.964209.

Weiner, O.H., Zoremba, M., Gressner, A.M., 1996. Gene expression of syndecans and betaglycan in isolated rat liver cells. Cell Tissue Res. 285 (1), 11–16.

Wilkening, S., Stahl, F., Bader, A., 2003. Comparison of primary human hepatocytes and hepatoma cell line Hepg2 with regard to their biotransformation properties. Drug Metab. Dispos. 31 (8), 1035–1042. http://dx.doi.org/10.1124/dmd.31.8.1035.

Xu, J.J., Henstock, P.V., Dunn, M.C., Smith, A.R., Chabot, J.R., de Graaf, D., 2008. Cellular imaging predictions of clinical drug-induced liver injury. Toxicol. Sci. 105 (1), 97–105. http://dx.doi.org/10.1093/toxsci/kfn109.

The use of metabolising systems for in vitro testing of endocrine disruptors. OECD, 2006. <http://www.oecd.org/chemicalsafety/testing/36280446.pdf>.